Escola Tècnica Superior d'Enginyers
de Camins, Canals i Ports de Barcelona
UNIVERSITAT POLITÈCNICA DE CATALUNYA

PROJECTE O TESINA D'ESPECIALITAT

Títol

BARCELONA BASIC MODEL: DETERMINATION OF THE SATURATED PRECONSOLIDATION STRESS

Autor/a

OLIVER TEALL

Tutor/a

ANTONIO LLORET

Departament

DEPARTAMENT D'ENGINIYERIA DEL TERRENY, CARTOGRAFICA I GEOFISICA

Intensificació

ENGINYERIA DEL TERRENY

Data

JUNY 2011

Abstract

Subject*: Barcelona Basic Model: Determination of the saturated preconsolidation stress*
Author: Oliver Teall
Tutor: Antonio Lloret

The behaviour of partially saturated soils has previously been modelled in ways that separate their fundamental features, and the formulation of a unifying model has been somewhat of a challenge. This paper looks to expand and give evidence towards the Barcelona Basic model (BBM) expressed in the paper 'A constitutive model for partially saturated soils' put forward by E. E. Alonso, A. Gens and A. Josa in 1990.The model gives a basic framework for the prediction of the behaviour of partially saturated soils that are slightly or moderately expansive in both isotropic and triaxial stress states.

The original paper is written with reference to the framework of hardening plasticity, and uses two independent sets of stress variables: the excess of total stress over air pressure and the suction. In fully saturated conditions, the model becomes a conventional critical state model, making it completely compatible with standard behavioural theory.

This thesis focuses on the change in preconsolidation stress of a clayey silt when fully saturated, with varying moisture contents and dry densities in triaxial state conditions. The results are used to 'map' these values in terms of their dependent variables and determine any graphical relationships that may exist between them.

The importance of this parameter is explained, particularly in reference to the predictive capabilities of the BBM. The reasons for the possible existence of a relationship between the preconsolidation stress and the soil's initial conditions are explained based on modern theory of soil mechanics.

Proctor compaction tests and triaxial state compression tests are used to find useful data for comparison. The tests undertaken, including all equipment and methods used are described in detail. The procedures for the collection of data are explained, and justifications given to any assumptions or simplifications made.

The results of the testing process are input into calculation spreadsheets to produce useful graphical interpretations with the intention of intelligently reviewing any existing relationships. The permeability of each sample is calculated from the data collected.

The impact of the change in void ratio associated with the preparation and saturation of the samples is investigated. The process and formulas used are explained.

The results are analysed and conclusions drawn regarding any existing relationships. The results are a basis onto which further tests using varying degrees of saturation can be added to in order to create Loading Collapse (LC) curves to demonstrate the theory put forward in the original model.

Included parameters

p = mean stress (kPa)
p'= effective mean stress (kPa)
p_o= preconsolidation stress (kPa)
p^*_o = saturated preconsolidation stress (kPa)
q = deviatoric stress (kPa)
σ = total stress (kPa)
λ = gradient of virgin compression line
u_a = air pressure (kPa)
u_w = water pressure (kPa)
δ = Kronecker delta
Sr = saturation ratio
w = moisture content (%)
ρ_d = dry density (g/cm^3)
κ = gradient of recompression line

Resume

Tema*: Barcelona Basic Model: determinación del estrés de preconsolidación*
Autor: Oliver Teall
Tutor: Antonio Lloret

El comportamiento de los suelos parcialmente saturados se ha modelado previamente de manera independiente con respecto a sus características fundamentales, con dificultades en la formulación de un modelo unificado. El propósito de este artículo es expandir y dar evidencia para el modelo expresado en el artículo previo 'A constitutive model for partially saturated soils' presentado por E. E. Alonso, A. Gens y A. Josa en 1990, que propone una estructura básica para modelar el comportamiento de suelos parcialmente saturados que son expansivos ligera o moderadamente en estados isotrópicos y triaxiales.

El artículo original está formado con referencia al marco de endurecimiento de la plasticidad, con 2 conjuntos de variables de estrés independientes: el exceso de estrés total sobre la presión del aire y la succión. En condiciones totalmente saturadas, el modelo conforma un modelo convencional de estado crítico, haciéndolo totalmente compatible con la teoría de comportamiento estándar.

El enfoque de esta tesina es en el cambio del estrés de preconsolidación de un limo arcilloso en condiciones saturadas con distintas humedades y densidad secas en estado triaxial. Se usan los resultados para presentar estos valores con respecto a sus variables dependientes y determinar gráficamente la relación entre sí.

La importancia de este parámetro se explica, especialmente con referencia a la capacidad predictiva del BBM. Las razones de una posible relación existente entre el estrés de preconsolidación y las condiciones iniciales del suelo se explican basadas en la teoría moderna de mecánicas del suelo.

Se usan ensayos de compactación de Proctor y de compresión en estado triaxial para conseguir datos útiles para la comparación. Los ensayos, el equipo y los métodos usados se describen a detalle. Se explican los procesos para la colección de datos y se justifican algunas suposiciones o simplificaciones.

Se redactan los resultados de los procesos del ensayo en hojas de cálculo para producir interpretaciones graficas útiles, con la intención de conseguir alguna relación existente. La permeabilidad de cada muestra se calcula a partir de los datos recogidos.

Se investiga el impacto del cambio del índice de poros asociados con la preparación y la saturación de las muestras, y se explican los procesos y formulas empleados.

Se analizan los resultados y se forman conclusiones con respecto a algunas relaciones existentes. Los resultados son una base en que se puede añadir ensayos adicionales que utilicen distintos grados de saturación para crear curvas de Loading Collapse (LC) para demostrar la teoría del modelo original.

Parámetros incluidos

p = presión medio (kPa)
p'= presión medio efectivo (kPa)
p_o= presión de preconsolidación (kPa)
p^*_o = presión de preconsolidación saturada (kPa)
q = presión desviadora (kPa)
σ = estrés total (kPa)
λ = gradiente de la línea de compresión virgen
u_a = presión del aire (kPa)
u_w = presión del agua (kPa)
δ = Kronecker delta
Sr = grado de saturación
w = humedad (%)
ρ_d = densidad seca (g/cm^3)
κ = gradiente de la línea de recompresión

Acknowledgements

I would firstly like to thank Rodrigo Gomez for his help and patience in the lab, as well as all the work he contributed towards this paper.

To my thesis tutor, Antonio Lloret, for pointing me in the right direction.

To José and Victor for all the assistance they provided

To my beautiful girlfriend Adriana, for her love and support throughout, and to my friends Jon, Jos and Vita for struggling through with me.

Table of Contents

Index of Figures

1

Index of Tables

Index of formulas

1 INTRODUCTION AND BACKGROUND THEORY

The Barcelona Basic Model (BBM), as described in 'A constitutive model for partially saturated soils', has been formed using well established concepts of hardening plasticity theory, and reduces to a critical state model when in fully saturated conditions.

The model looks to describe the behaviour of moderately expansive soils such as sands, silts, clayey sands, sandy clays and clays of low plasticity in partially saturated conditions, in order to more comprehensively understand the effect of changes in suction (defined as the difference between air pressure u_a and pore pressure u_w) on the behaviour of the soils in different loading conditions. The overall aim of the model is to be able to provide a simple general framework to explain and predict the soils' behaviour in partially saturated conditions.

The model uses the three stress states: $(\sigma_{ij} - u_a\delta_{ij})$; $(\sigma_{ij} - u_w\delta_{ij})$ and $(u_a - u_w)\delta_{ij}$ to describe the stress-strain-strength behaviours, where σ_{ij} is the total stress and δ_{ij} the Kronecker delta.

Suction contributes to stiffening the soil against external loading, and changes in suction may induce irreversible volumetric deformations. These volumetric changes depend on the initial and final stress and suction values, as well as the particular stress path followed. For this reason the creation of a comprehensive model requires both theoretical and experimental evidence from many different testing conditions before becoming truly useful.

The partially saturated behaviour of the soils is described in part via the creation of Loading Collapse (LC) curves to model the change in preconsolidation stress p_o with suction.

The results and conclusions given in this thesis are to supplement the existing experimental evidence for the Barcelona Basic Model. This is to be done by investigating the possible existence of graphical relationships for the changes in saturated preconsolidation stress p^*_o with varying moisture contents and dry densities (the two being themselves related) in fully saturated conditions in order to then map out these changes as part of the 'critical state' section of the original model. It is expected that these results be built upon following experiments with varying levels of suction to provide further evidence to the model, which may then be seen to take into account the initial conditions of moisture content and dry density in predicting soil behaviour.

The preconsolidation stress parameter p_o is important as it determines the boundary of the yield surface on the (p, q) stress plane, that is to say the point at which the soil begins to behave plastically, and can be defined for changing levels of suction. It is this change in p_o with suction that is modelled by the LC curve that the BBM looks to predict accurately. The curves show how with increasing levels of suction, the preconsolidation stress increases and therefore the yield surface expands, up to a yield locus or 'suction increase' (SI) surface.

The change in preconsolidation stress with changes in mean stress defines the plastic behaviour of the soil. The BBM considers only hardening plasticity, with an increasing yield surface due to loading (attributed to Normal and Slightly Over-consolidated soils) and therefore increasing values of preconsolidation stress.

The value of the initial preconsolidation stress p^*_0 in saturated conditions defines the initial position of the yield surface and the start of plastic behaviour when the degree of saturation Sr = 1, which is the starting point for the LC curve in the BBM model. Depending on the initial moisture content and dry density of the soil, the initial preconsolidation stress and therefore the initial yield surface will differ. This paper looks to attempt to define the relationship between these changes in values for the initial preconsolidation stress via proctor compaction tests and triaxial state experimentation in saturated conditions and gives reasoning and analysis to the results, for further use in the BBM.

1.1 Background theory

The preconsolidation stress parameter describes the maximum previous effective stress state encountered by the soil, and affects hugely its behaviour under new loading.

The reason for these effects lies in soil mechanics theory of settlements. A soil is 3-phase: solid, liquid (water) and air. These phases are measured in terms of volumes and weights to allow the definitions of standard soil mechanics properties.

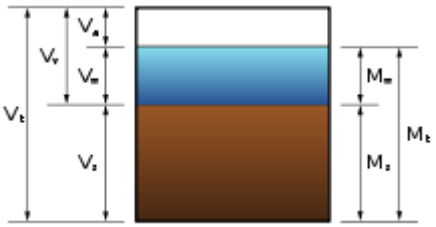

Figure 1.1.1: *Typical 3-phase diagram of soil*

The soil properties considered in this thesis are:

(1)

$$water\ content\ (w) = \frac{M_w}{M_s}$$

(2)

$$dry\ density\ (\rho_d) = \frac{M_s}{V_t}$$

(3)

$$void\ ratio\ (e) = \frac{V_v}{V_s}$$

(4)

$$saturation\ ratio\ (S_r) = \frac{V_w}{V_v}$$

(5)

$$porosity\ (n) = \frac{V_v}{V_t}$$

(6)

$$specific\ gravity\ (G_s) = \frac{\gamma_s}{\gamma_w}$$

This thesis considers only saturated conditions, in which the saturation ratio $S_r = 1$. These conditions mean that all voids within the soil are occupied by water; therefore, the volume of voids is equal to the volume of water, as shown in figure 1.1.2. This characteristic is used to measure the volumetric deformation via the measurement of expelled water from the sample during the triaxial compression stage.

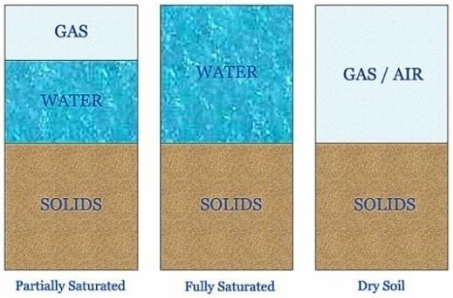

Figure 1.1.2: *Phase diagrams of soil in different moisture-related conditions*

When subjected to a high enough load, the volume of voids of the soil decreases, either through compaction (reduction of air) if unsaturated, or consolidation (reduction of water). The volume of the soil itself doesn't change, making the void ratio (V_v/V_s) decrease.

The deformations experienced by the soil can be described as elastic or plastic. For a theoretical soil that has not previously been subjected to any loading, all loading would be plastic. This is as no permanent reduction of void spaces has previously occurred, and therefore any loading would initiate this change.

Any real soil, however, will have previously experienced loading which has acted to reduce the initial void ratio to some extent. Depending on the current stress state of the soil and its maximum previous stress state, a soil can be described as normally consolidated (the current stress state is the maximum that the soil has experienced) or over consolidated (soil has experienced previous, higher stress states).

The experiments detailed in this paper are with regards to normally or slightly over-consolidated soils, and are to be tested from a low stress state, to allow a reconsolidation path to be followed (and therefore the obtention of the parameter κ) before the preconsolidation stress is reached.

Figure 1.1.3 shows the standard graphical presentation of this behaviour. The recompression line demonstrates how stress may be applied to the sample without causing much change in void ratio, as previous stresses have already caused a permanent change.

Point c on the graph indicates the point at which the soil begins to follow plastic deformation behaviour. The value of stress at this point is taken as the preconsolidation stress, and the void ratio at this point will be equal to the void ratio at the previous highest stress state experienced by the soil.

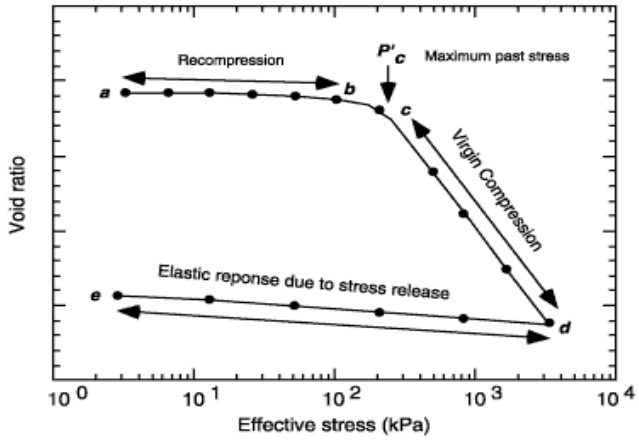

Figure 1.1.3: *Standard graphical representation of the virgin and recompression lines*

For this reason, the preconsolidation stress largely affects the deformations experienced by a soil under new loading, and particularly the point at which these deformations and settlements become plastic.

As part of the analysis of the results of the testing, the values found for void ratios are altered slightly to investigate the change in void ratio due to the soil trimming and saturation process. This is achieved via back-calculation of void ratio using the final value (which will be accurate) and the measured deformation of the soil.

The formula used to carry out these corrections is from standard soil mechanics theory:

(7)

$$\varepsilon_{vol} = \frac{\Delta e}{(1 + e_0)}$$

Rearranged:

(8)

$$e = e_0 - \varepsilon_{vol} \cdot (1 + e_0)$$

This back-calculation is undertaken to see whether the alteration of the results is necessary in terms of finding graphically the preconsolidation stress.

The preconsolidation stress defines, in the p-q plane, the surface at which the soil behaviour changes from elastic to plastic, and specifically is the value of mean stress on the point of the yield surface at which the deviatoric stress q is equal to 0.

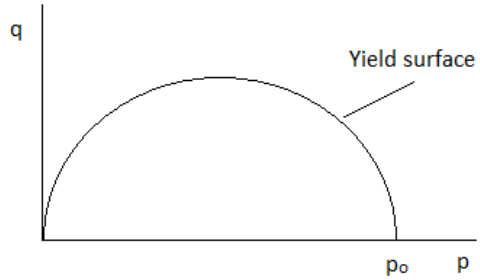

Figure 1.1.4: *Preconsolidation stress in p-q plane*

As the Barcelona Basic Model is formulated within the framework of hardening plasticity, only the increase in p_o is being considered. The model aims to predict plastic behaviour of partially saturated soils by defining a yield surface in the p-q-s plane, modelling the increase in preconsolidation stress with suction.

This model is created via the initial formation of LC curves in the p-s plane that describe the increase in p_o with suction, then later mapping this curve onto the 3d stress space, including the limit of increase in suction, as shown in figure 1.1.5.

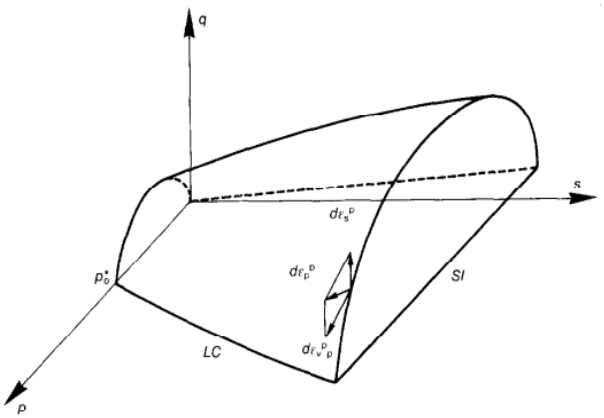

Figure 1.1.5: *Three-dimensional view of the yield surface in (p, q, s) stress space*

For the formation of these LC curves, it is necessary to test soils at various levels of suction, that is to say various grades of saturation. The logical starting point for the LC curve is the attainment of the saturated preconsolidation stress p^*_o, which in itself varies with differing initial moisture content and dry density of the soil. It is therefore important to be able to define how this value changes in order to predict it accurately.

The preconsolidation stress is found for soils subjected to proctor compaction tests of differing energies with moisture contents below, similar to and above the specific optimum, using triaxial state testing and graphical interpretation. These changes in preconsolidation stress are compared for differing initial conditions in order to successfully analyse the parameter's dependency on them.

The relationship between dry density and moisture content is already well known through Proctor compaction test results. Theoretically, the preconsolidation stress parameter only depends on the previous stress state experienced by the soil, which affects the initial void ratio. However, the BBM shows how this value changes with changes in the degree of saturation (i.e. changes in suction). It is suspected that some direct relationship may exist between the moisture content and dry density variables, and the preconsolidation stress. The purpose of this paper is to investigate this possibility.

2 OBJECTIVES

2.1 Principal

The purpose of the paper is to investigate the possibility of a graphical relationship between the saturated preconsolidation stress p^*_o and varying moisture contents w and dry densities $\rho_{d.}$ Any existing relationship is determined and backed up by theoretical reasoning. The results are then related back to the Barcelona Basic Model defined by E.E. Alonso, A. Gens and A. Josa.

2.2 Extended

The extended purpose of the paper and the tests it involves is to provide experimental evidence and data to allow the more accurate modelling of the initial yield surface (in saturated conditions) for moderately expansive soils with the intended purpose of the further modelling of the soils in partially saturated conditions using the complete BBM.

The paper is intended in general as an addition to the current experimental data for the Barcelona Basic Model, and its results and conclusions should be seen therefore to relate to it.

3 METHODOLOGY

To determine accurately the relationship $p^*_o(w, \rho_d)$ between the saturated preconsolidation stress and both the moisture content and dry density of the clayey silt, both proctor compaction tests and saturation – loading tests in triaxial conditions are used.

3.1 Type of soil

The soil from which the samples are taken is a clayey silt used in experimental embankment works and taken from the A-28 motorway in Rouen.

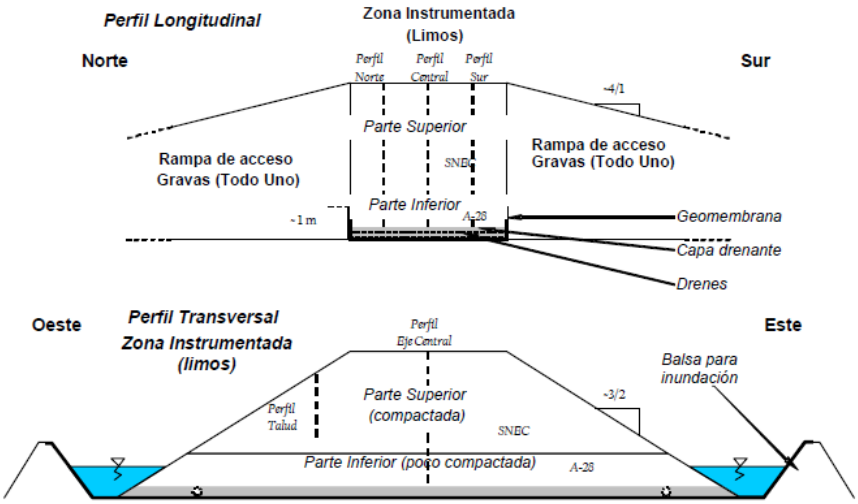

Figure 3.1.1: *Longitudinal and transverse profiles of experimental embankment*

The soil is from the inferior (lightly compacted) section. The soil contains around 95% fines, with 23% clay.

Figure 3.1.2: *The A-28 clayey silt being used in the construction of the embankment*

Further properties of the soil, and the individual initial conditions for each sample used in the testing process are detailed later.

3.2 Tests carried out

Two proctor compaction methods are used to prepare the sample for triaxial testing: full-force/standard proctor and half proctor. The compaction curves showing the relationship between the moisture content and the dry density are derived for each of the two compaction tests, and compared to show their relationship. From the curves, the optimum moisture content for each is located graphically. Figure 3.2.1 shows the standard representation of the results for a proctor compaction test.

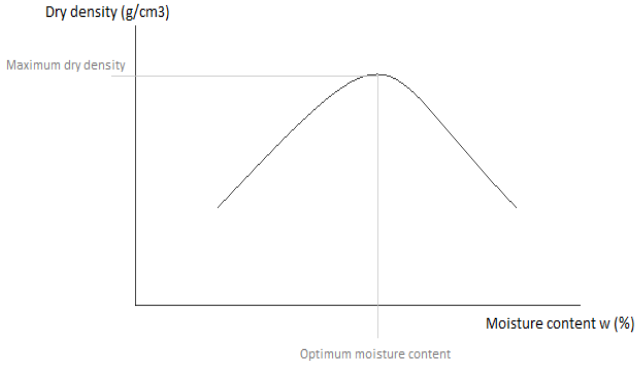

Figure 3.2.1: *Typical graphical results of standard Proctor test*

For each of the proctor curves, samples are compacted at moisture contents lower than, similar to and higher than the optimum for use in triaxial testing, in order to fully determine the effect of compaction on the 'dry' and 'wet' sides on the preconsolidation stress.

The samples are first saturated fully in the triaxial apparatus to ensure their compliance with standard critical state behaviour, and subsequently compressed isotropically to levels surpassing the preconsolidation stress caused by the compaction process.

The results of this isotropic compression are presented graphically on axes of void ratio against applied stress (the latter being displayed logarithmically) and deformation against applied stress. The graphs show first the recompression relationship of the soil (with stress levels below p_o) displayed by a line of gradient κ, which changes to the virgin compression line of gradient λ after reaching and exceeding the preconsolidation stress, as shown in figure 1.1.3. These parameters are determined for each test to fully analyse the soil response.

Each of the tests are compared graphically and in terms of their relationship parameters to gain an understanding of the effect of changes in initial conditions on the preconsolidation stress parameter.

The original intention was to carry out at least 4 tests using both the standard Proctor compaction method and the half-force Proctor compaction method. However, due to a string of issues faced during testing, it was possible to complete 4 tests for the standard Proctor compaction, but only 2 for the half Proctor. All the results collected will be shown and analysed, but further testing may be required before a full conclusion can be given.

3.3 Equipment used

The Proctor compaction process is carried out using standard proctor equipment consisting of a 2.495kg weighted hammer and a cylindrical brass mould with a capacity of 0.00094m³. Further equipment used in the procedure as a whole includes an accurate scale (sensitive to 0.5 grams), a micrometre for accurate dimension measurements and drying equipment in the form of a large oven capable of maintaining a temperature of 110˚C ($^{+}_{-}$ 5˚C).

Figure 3.3.1: *Proctor compaction equipment - Compaction hammer and cylindrical container*

The triaxial saturation and compression which proceeds the proctor compaction is carried out using a triaxial cell connected to digital pressure controllers filled with water (used to inflict isotropic stress changes to the sample) and computer monitoring software (to log the research data at set time intervals)

Figure 3.3.2: *Triaxial cell*

Two pressure controllers are used, capable of inducing large, controlled pressure changes to the triaxial cell; one to induce an increase in cell pressure, creating an isotropic increase in stress in the mounted sample, and a second to force water through the sample, ensuring its saturation and allowing the measurement of the sample's permeability.

Figure 3.3.3: *GDS digital pressure controller*

The computer monitoring software used is GDSLAB, a programme that allows the logging of data and automatic creation of graphs in real-time. This data is later taken and used to find important soil parameters and analyse any existing relationships.

3.4 Testing procedure

The procedure for the testing of the clayey silt begins with the crushing of the soil into particles of diameter smaller than 2mm using a simple 'hammer and bucket' approach and using a standard no.10 sieve.

Once crushed, 2kg of the soil is used in the compaction process. The hydroscopic moisture content is measured by taking a small sample and comparing weights before and after drying. From the result, and depending on the desired water content for the test being carried out, water is added to the sample, ensuring the most uniform mix possible is achieved.

The sample is then compacted in the cylindrical container following standard Proctor compaction test procedures, using either 25 hammer drops of 300mm height (for standard Proctor) or 13 hammer drops of 300mm height (for half-Proctor), rotating the position of the impacts relative to the soil sample after every blow to ensure relatively uniform compaction.

The sample is weighed and extracted from the container, then trimmed down to a 50mm or 38mm diameter sample using a hand-operated soil trimmer.

Figure 3.4.1: *Hand-operated soil trimmer*

These diameters are chosen to match the standard diameter of the triaxial cell equipment being used. The sample is also cut down vertically to up to half of its original height, to allow faster saturation in the triaxial machine. This sampling procedure results in a compacted cylindrical soil sample of diameter 50mm or 38mm ($^{+}_{-}$0.5mm) and height ranging between 50mm and 65mm (the cross-sectional area and height of the sample are taken into account in calculations, so large variations do not affect the results).

The compacted sample is placed in the triaxial machine, using two membranes along the sample's length, along with filters and porous discs at either end to ensure the vertical flow of water through the sample, but restricting lateral flow into the cell chamber.

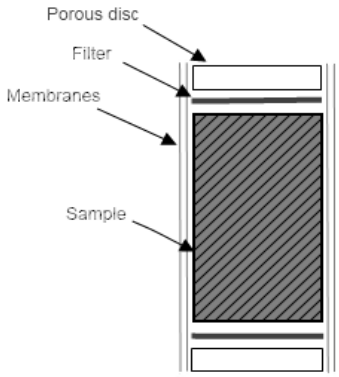

Figure 3.4.2: *Diagram showing arrangement of sample in triaxial apparatus*

Saturation is then achieved over the course of 1-2 days by forcing water through the sample, using a back pressure of 40kPa along with a cell pressure of 45kPa (to act against the 'bulging' of the sample during testing). This is done allowing the free flow of the water through the sample, without measurement of pore pressure.

After the initial 1-2 days, the free flow of water through the sample is halted, and the pore pressure is measured within the sample in order to ensure that saturation has been achieved (i.e. the pore pressure is equal to the back-pressure being applied)

Once saturated, the sample is subjected to an isotropic stress increase up to 1500KPa, to ensure that the preconsolidation stress is surpassed and that enough results are collected for a proper analysis to occur. This increase is applied in drained conditions to allow effective mean stress relationships to be derived (a very slow increase in stress allowing the exit of water from the sample).

The increase in stress and resulting increase in strain in the sample is measured using the computer equipment, as well as monitoring the pore pressure to ensure continued drained conditions. Theoretically, no change in pore pressure should be experienced by the sample, but some small increase is likely to be measured due to the low permeability of the samples.

3.5 Analysis of results

The test data is taken every 300 seconds (5 minutes) to ensure comprehensive results of the test are recorded.

The results from the proctor compaction tests are used to form graphs of dry density against moisture content. From these graphs the optimum moisture content and maximum dry density can be located, as well as the relationship between the two parameters for both standard Proctor compaction and half-force Proctor compaction.

The results of the triaxial compression tests are used to form graphs of both void ratio and volumetric deformation against stress (on a logarithmic scale). From these graphs, the preconsolidation stress can be found as the stress at which the gradient of the line changes significantly to follow the virgin compression line of gradient λ instead of the recompression line of gradient κ.

The results found are altered slightly using back-calculation to take into account the slight change in void ratio that will have occurred during the trimming and saturating phases. This is to investigate the need for the correction of the preconsolidation stress

value due to this small alteration. The altered results are plotted on graphs against the original recorded results to come to a conclusion.

The permeability for each sample is calculated via graphs of volume of water entering the sample against time. The flow rate through the sample is derived directly from part of the whole graph, and then used along with the individual dimensions of each sample to calculate the overall permeability.

The preconsolidation stress parameter from each test is plotted on graphs of both preconsolidation stress against moisture content and preconsolidation stress against dry density in order to determine graphically any relationship, and come to a considered conclusion.

Due to the nature of the results, it was necessary to come to several speculative conclusions to be built on in further experiments.

4 EXPECTED RESULTS

The tests undertaken produce a series of results as graphs in order to analyse the data.

4.1 Proctor compaction curves

The starting point is to create Proctor compaction curves, which indicate graphically the relationship between dry density and moisture content for the soil.

The standard Proctor test and the half-force Proctor test are expected to create slightly different curves, as with the standard and modified Proctor curves.

The modified Proctor test uses a mass of 4.54kg (10lbs) dropped from 45.7cm (18in) and compacts 5 layers in place of the normal 3. The compaction curve, therefore, will note higher dry densities for similar moisture contents, as shown in figure 4.1.1.

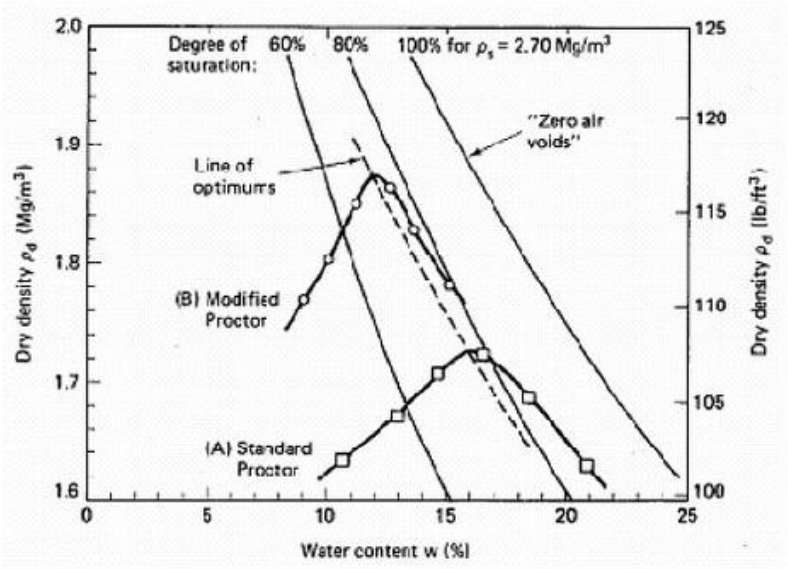

Figure 4.1.1: *Graph of Proctor compaction curves: Standard and Modified*

This relationship is seen because with higher energy compaction, the soil particles will be compacted more (with higher reduction in void space) and therefore experience an increase in the weight of the soil in terms of the total volume (the volume in which the soil is compacted is not changed, but the amount of soil that can be compacted is).

The same theory can be applied with the half-force Proctor in relation to the standard. The lower force should result in lower values for dry density for similar moisture contents.

4.2 Stress against void ratio / volumetric deformation

Once isotropic triaxial state compression testing has occurred, graphs of stress (plotted logarithmically) against void ratio and volumetric deformation can be created.

These graphs show how the force acts to consolidate the soil and expel water from the pores, reducing pore size and therefore void ratio over time. The reduction in void ratio is proportional to the volumetric deformation, so either can be used to find the necessary parameters.

The important parameters associated with the graphs are the preconsolidation stress, the gradient of the virgin compression line λ and the gradient of the recompression line κ.

It is expected that for each of the triaxial tests run, one of these graphs is created which will contain a short period of recompression followed by a noticeable change in gradient (showing the position of the preconsolidation stress) and a period of virgin compression.

The key to the paper is the analysis of the relationship between these graphs, and how in particular the location of the point of change of gradient occurs with respect to the initial conditions.

The results for preconsolidation stress are to be plotted separately against moisture content and dry density, in an attempt to find a useful relationship.

It would be expected that when saturated, the moisture content and the preconsolidation stress follow an inverse relationship. This is because, as explained earlier, in saturated conditions all the void spaces within the soil are filled with water, making any change in volume of voids equal to the change in the volume of water.

As a result of this, with higher preconsolidation stress, the weight of the water in relation to the weight of the solids for a given volume of soil would be lower, as a lower volume of voids, equal to the volume of water in saturated conditions, would exist in comparison with the volume of solids present. As the moisture content is defined by the mass of the water divided by the mass of the solids (equation 1), this should result in a relationship of the type shown in figure 4.2.1.

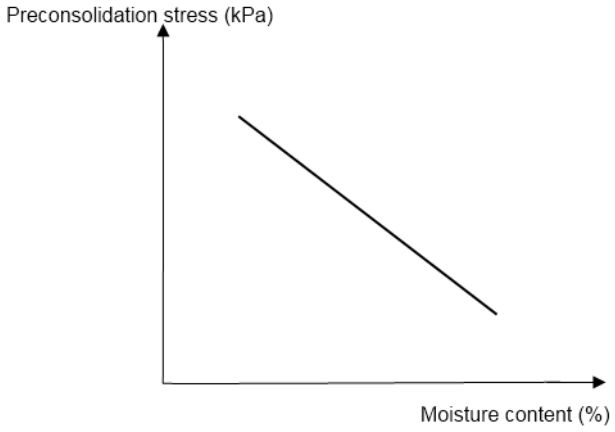

Figure 4.2.1: *Theoretical relationship between preconsolidation stress and moisture content in saturated conditions*

In contrast, with respect to the dry density of the soil, the preconsolidation stress would be expected to be higher with higher values for dry density in saturated conditions. This is because with a higher previous stress state, the mass of the solids within the soil should be higher with respect to the overall volume. In this case, the volume is fixed, and it is only the quantity of solids compacted into that volume which varies.

As the dry density is defined by the mass of solids divided by the total volume (equation 2), this value will theoretically increase with larger preconsolidation stress, as shown in figure 4.2.2.

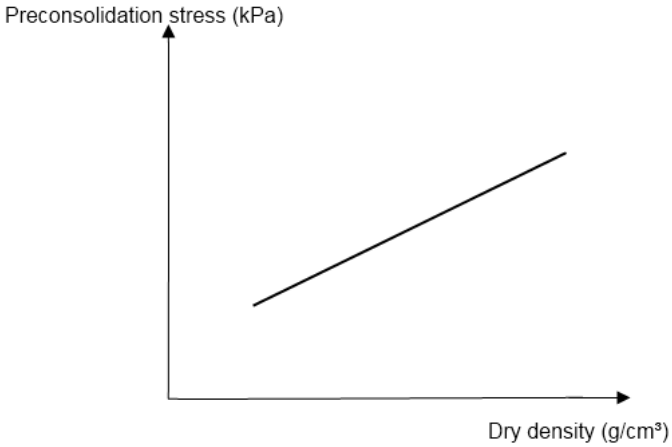

Figure 4.2.2: *Theoretical relationship between preconsolidation stress and moisture content in saturated conditions*

5 RESULTS

5.1 Proctor compaction tests

To determine the initial relationship between moisture content and dry density, the values from the Proctor compaction tests are taken and compared.

5.1.1 Standard Proctor test

Four separate samples were prepared using the standard Proctor method. For each of these samples the moisture content was measured using mass measurements of samples before and after heating in an oven of heat 110°C for over 24 hours with the difference in mass being taken as the mass of water in the sample.

The dry density was calculated using the total mass of the sample in the Proctor mould, subtracting the mass of the mould itself and dividing by the total volume (1000cm³).

Standard Proctor		
Test	w	ρ_d
3	15.84	1.7710
1	16.25	1.7732
2	16.76	1.7450
4	17.07	1.7357

Table 5.1.1 *Standard Proctor test sample data*

(The numbering of the tests is purely chronological and is for reference purposes only)

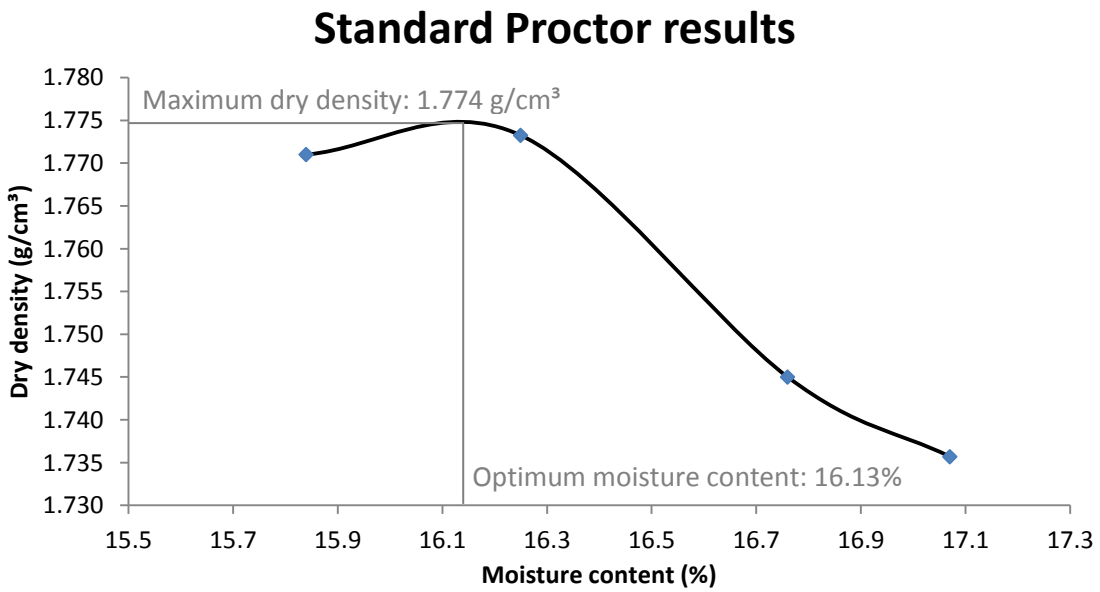

Figure 5.1.1: *Standard Proctor test graphical results*

Figure 5.1.1 showing the results of the Standard Proctor test on axis of moisture content against dry density show a clear optimum moisture content of around 16.13%, and a maximum dry density of 1.774g/cm³.

The moisture content and dry density values for each of the samples will be used later to compare against preconsolidation stress value.

Each of the samples was also compressed in triaxial conditions to create graphical results for effective mean stress against volumetric deformation and void ratio.

From figure 5.1.1 it can be seen that one sample has been taken on the ‘dry’ side, two on the ‘wet’ side and one around optimum moisture content, to investigate the effect of the moisture content on the preconsolidation stress in relation to the optimum value.

5.1.2 Half-force Proctor test

To form the half-force Proctor compaction curve, five samples of differing moisture contents were used. The moisture content and dry density were measured using the same method as in the standard Proctor testing.

Half force Proctor		
Test	w	ρd
-	12.05	1.616
-	13.11	1.685
-	16.26	1.724
-	18.53	1.706
-	20.09	1.674

Table 5.1.2: *Half force Proctor test sample data*

The samples for the half-force Proctor test are not numbered as they were not used for the triaxial testing stage. Instead, separate samples were taken from along the curve to compress isotropically.

For the half-force Proctor compaction, the Proctor curve was formed separately and prior to any triaxial testing of the samples in order to locate the optimum moisture content, whereas in the standard Proctor compaction an estimate of the optimum was already available, so triaxial testing could coincide with the Proctor testing.

Figure 5.1.2 showing the half force Proctor test results shows a similar optimum to that of the standard Proctor, of around 16.4%. However, the maximum dry density can be seen to be lower, at around 1.725g/cm^3, a difference of 0.049g/cm^3. This difference is due to the lower compaction force and therefore less complete compaction of the soil, resulting in a sample of the same volume (equal to the volume of the Proctor mould) but lower mass of soil.

Using these curves, samples can be taken using various moisture contents and used in triaxial compression testing. For the standard Proctor test samples, those used to form the curved are used directly in the second stage of testing.

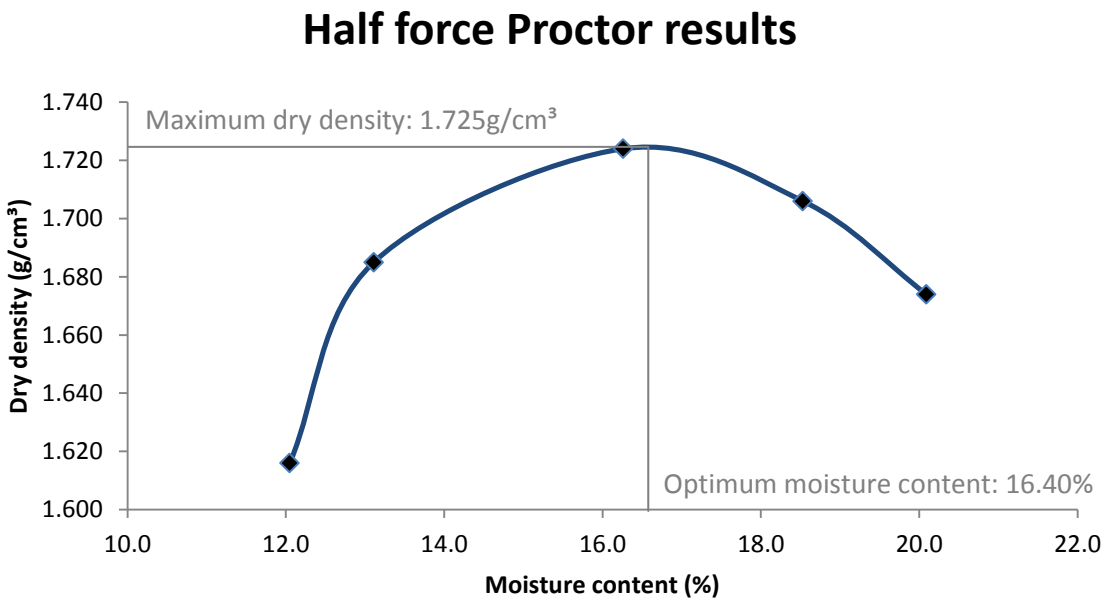

Figure 5.1.2: *Half force Proctor test graphical results*

Due to the time taken to isotropically load each sample and record the results, and the fact that the optimum moisture content needed to be located prior to any triaxial testing, this was not possible for the half-force Proctor test samples. Instead, two samples were taken of differing moisture contents for the half-force compaction and used in the triaxial testing. As explained earlier, this compromise was necessary due to several problems that arose during the testing process that resulted in there not being enough time to complete as many tests as was desired. From the tests run and results taken, as full analysis as possible is carried out.

5.2 Triaxial compression

For Triaxial compression testing, four samples were compacted using the standard Proctor method, and two using the half-force Proctor method. All samples were first saturated for 1-2 days with a constant cell pressure of 45kPa and back pressure of 40kPa.

Following saturation in which free flow of water was permitted through the sample, the pressures were maintained while the valve allowing the exit of the water from the sample was closed. The pore pressure was then measured over the course of one day to ensure saturation had been achieved and that the measured pore pressure equalled the applied back pressure.

A slow isotropic pressure ramp was applied to allow drained conditions to ensue. The reaction of the sample to the compression process was recorded, and data organised to present the results in useful graphical format.

The results are more useful if split into the two separate compaction methods.

5.2.1 Standard Proctor

5.2.1.1 Test 1

The initial conditions for the first sample used in triaxial testing are as follows:

Sample 1 Data Initial Conditions	
Height H_o (mm)	100.55
Volume V_o (mm^3)	197271.55
Cross-sectional area (mm^2)	1961.92
Weight of soil (g)	409.43
Specific Gravity G_s (g/cm3)	2.66
Natural density (g/cm^3)	2.08
Dry density (g/cm^3)	**1.77**
Moisture content w (%)	**16.25**
Volume of Solids Vs (mm^3)	131507.52
Volume of Voids Vv (mm^3)	65764.03
Void ratio	0.5001
Vw (mm^3)	56844.13
Degree of Saturation Sr (%)	86.44

Table 5.2.1: *Test 1: Initial conditions*

To analyse the results of the triaxial testing, the results can be plotted on a graph of effective mean stress against volumetric deformation. The preconsolidation stress p_0 can be found as the stress at which the extended gradient lines from each section of the graph cross.

The gradients of the two lines, recompression and virgin compression, are given as kappa and lambda respectively, and indicated on the graph.

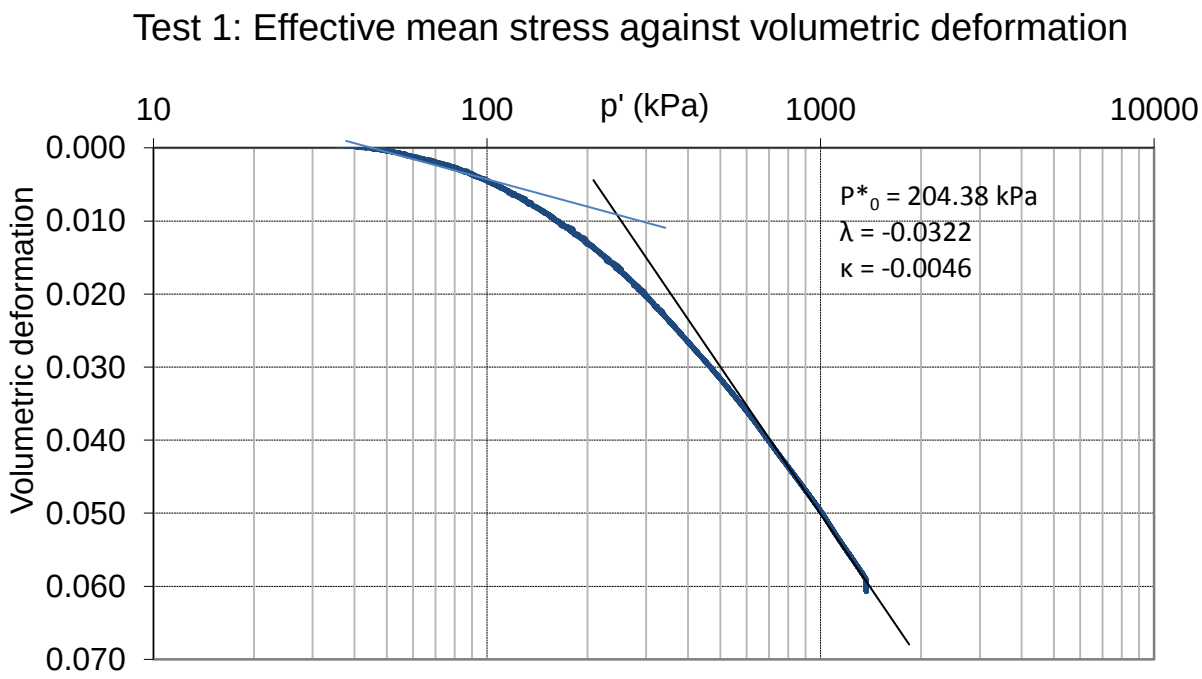

Figure 5.2.1: *Test 1: Effective mean stress against volumetric deformation*

From the results recorded, a graph of void ratio against mean effective stress can be plotted. However, the data began recording changes in void ratio only after the initial saturation process under a constant stress of 45kPa. This constant stress will have caused a slight change in void ratio due to the gradual consolidation of the soil. It is therefore necessary to calculate this initial change via the back-calculation method described earlier, to create a second curve or effecti
ve mean stress against void ratio.

The two curves are shown in figure 5.2.1. The blue curve shows the original recorded values, and the red curve those that were back-calculated using formula 8. The difference in initial void ratios can be taken as the consolidation due to trimming and saturation.

This change in void ratio due to trimming and saturation is calculated as around 0.0615. This value is comparatively small but could be seen as significant in terms of void ratio itself. However, the effect is has on the preconsolidation stress parameter, as shown by figure 5.2.2, is negligible and can be ignored. This can be seen as the point at which the two gradient lines cross is only altered along the y-axis, in terms of void ratio, and not along the x-axis, in terms of mean stress. Therefore the preconsolidation stress value does not change.

For comparison purposes, the graphical parameters for test 1 are:

λ	**κ**	**P_o^***
-0.0322	-0.0046	204.38 kPa

Table 5.2.2: *Test 1: Parameters of graph of results*

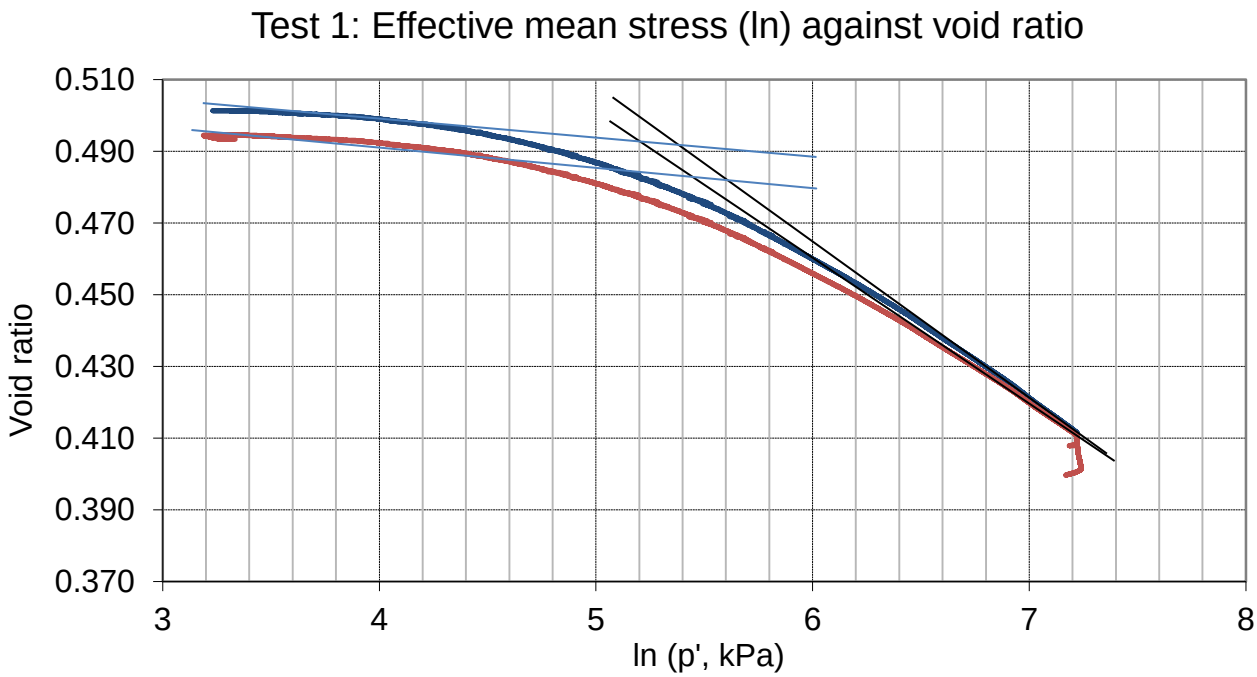

Figure 5.2.2: *Test 1 - Effective mean stress (ln) against Void ratio*

Figure 5.2.3 below describes the changes in mean stress, effective mean stress, water pressure within the sample and the volume of water being used for the testing process in test 1.

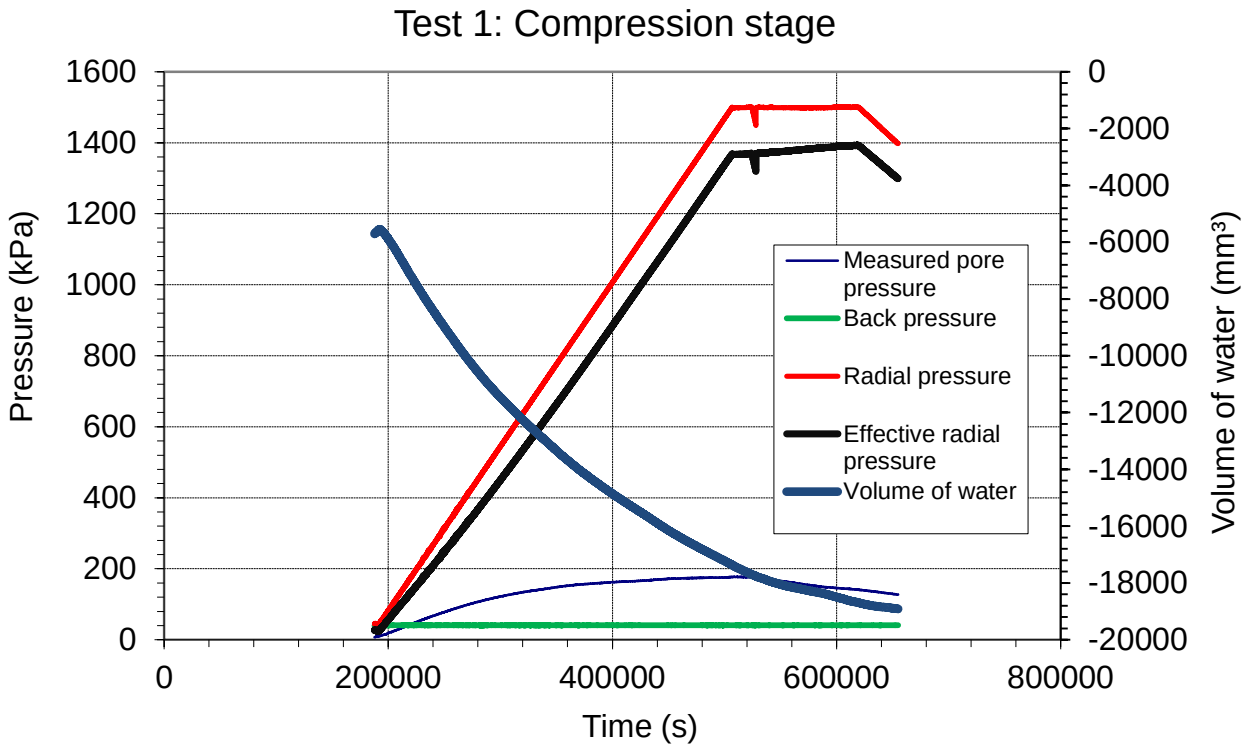

Figure 5.2.3: *Test 1: Compression stage process*

For test 1, the full pressure ramp up to 1500 kPa was applied and maintained for a period of time. As can be seen from the pore pressure measurements as well as the difference between the total and effective radial pressures, there was some increase in pore pressure during the compression process.

This signifies that ideally a slower pressure ramp should be applied in order to model fully drained conditions. However, this would have made the testing process significantly longer, creating added difficulties in obtaining sufficient results. For this reason it was decided to use the effective pressure values and therefore effective mean stress values calculated from incremental differences between total radial pressure and pore pressure in the results in order to take this increase in pore pressure into account.

5.2.1.2 Test 2

Initial conditions of test 2:

Sample 2 Data Initial Conditions	
Height H_o (mm)	62.50
Volume V_o (mm³)	122718.46
Cross-sectional area (mm²)	1963.50
Weight of soil (g)	240.00
Specific Gravity G_s (g/cm3)	2.66
Natural density (g/cm³)	1.96
Dry density (g/cm³)	**1.75**
Moisture content w (%)	**16.76**
Volume of Solids Vs (mm³)	77067.67
Volume of Voids Vv (mm³)	45650.79
Void ratio	0.59
Vw (mm³)	34358.00
Degree of Saturation Sr (%)	75.26

Table 5.2.3: *Test 2:Initial conditions*

Test 2 is of a sample of slightly higher moisture content (on the 'wet' side of the optimum) and with a slightly lower dry density. Figure 5.2.4 shows the effective mean stress and volumetric deformation relationship for this test.

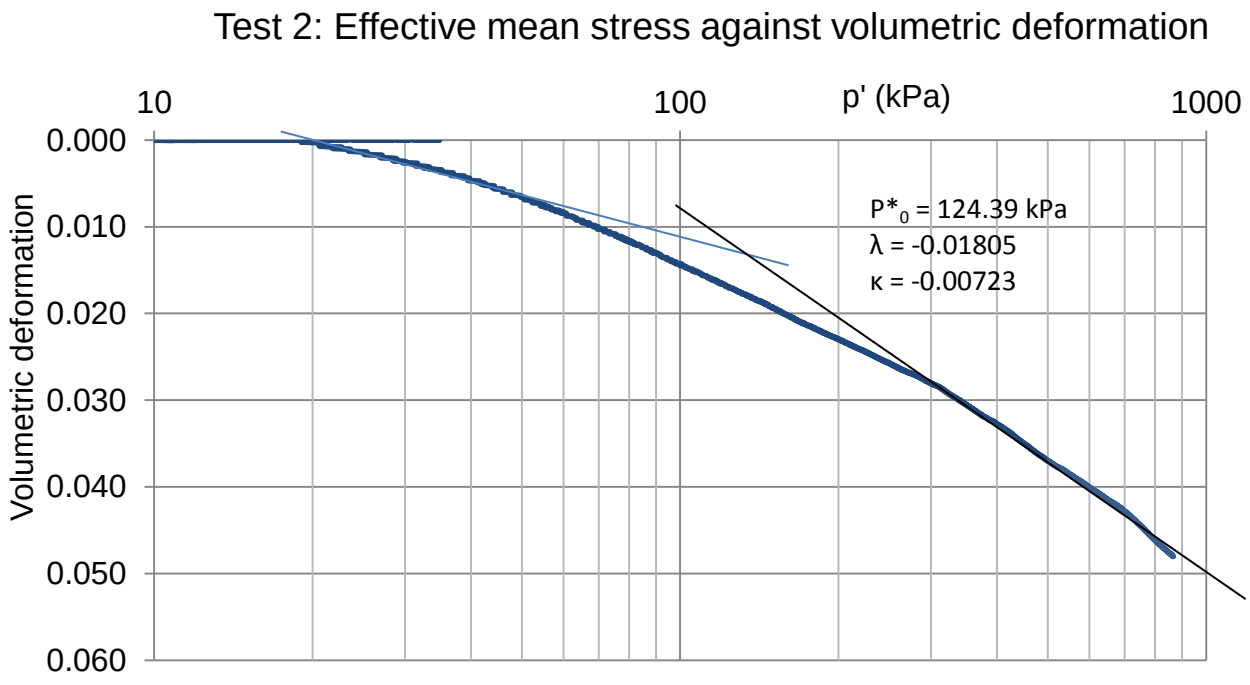

Figure 5.2.4: *Test 2: Effective mean stress against volumetric deformation*

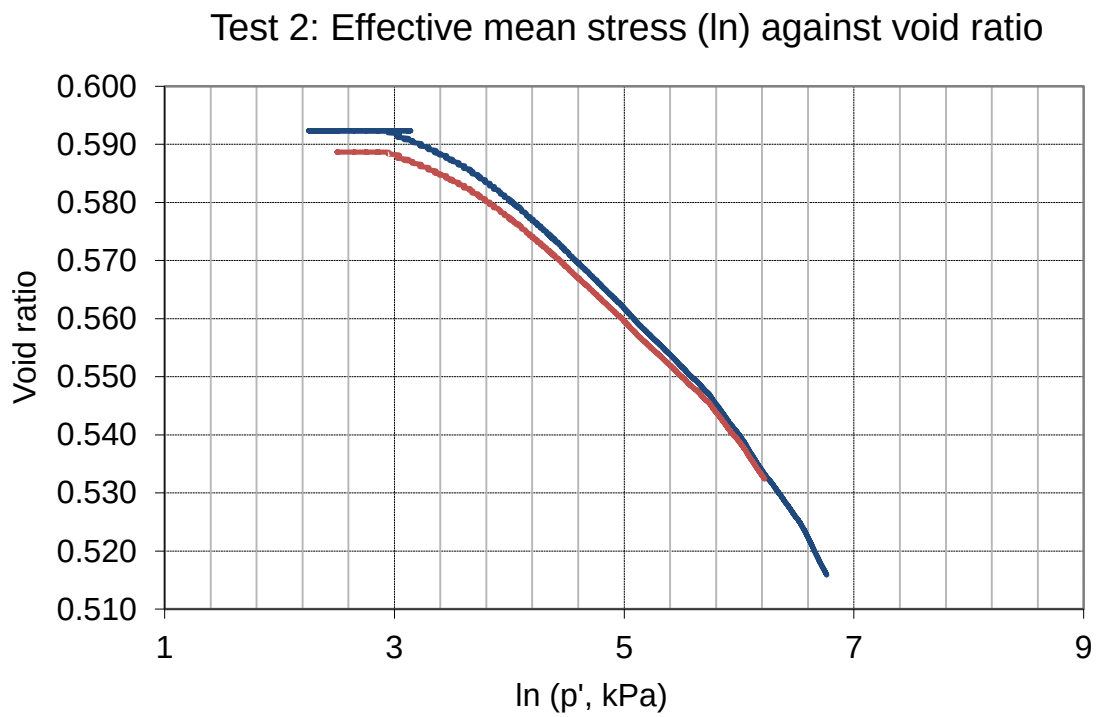

Figure 5.2.5: *Test 2: Effective mean stress (ln) against void ratio*

Figure 5.2.5 shows the change in void ratio due to trimming and saturation to be around 0.0037. This change is even smaller than for test 1, and so can also be ignored in terms of its impact on the preconsolidation stress for the same reasons.

Graphical parameters:

λ	κ	P_o^*
-0.01805	-0.00723	124.39 kPa

Table 5.2.4: *Test 2: Graphical parameters*

Table 5.2.4 shows the graphical parameters associated with test 2. The recompression slope for this test is lower than that of test 1, but gives a higher value for the virgin compression slope. The preconsolidation stress has been measured as much lower than that of test 1.

Figure 5.2.6 shows the triaxial compression process for test 2. As it was known that the preconsolidation stress would not exceed around 210kPa for the soil, the pressure ramp was not continued to the original 1500kPa, but instead the test stopped at a radial pressure of around 950kPa, deemed sufficient for the obtention of the necessary parameters.

As with test 1, some increase in pore pressure was measured, but not enough to cause any problems with using the effective mean stress values for analysis.

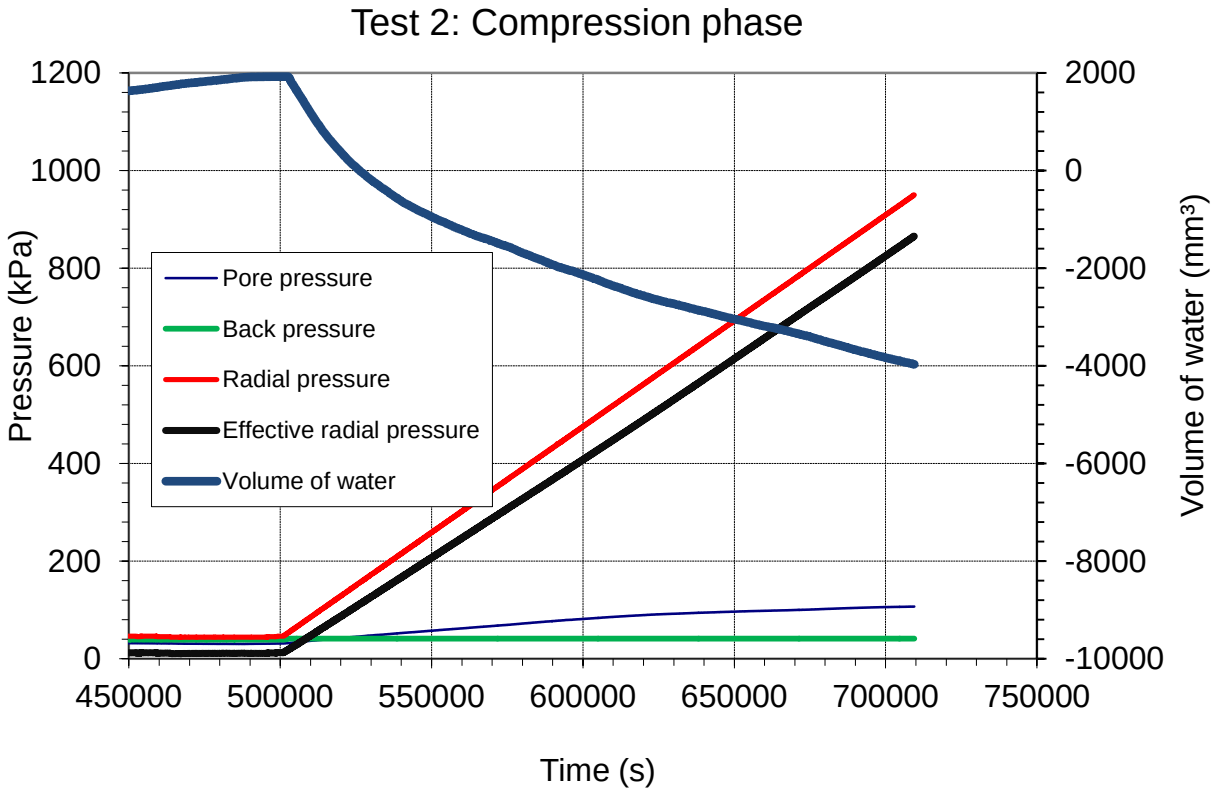

Figure 5.2.6: *Test 2: Compression phase process*

5.2.1.3 Test 3

Initial conditions of test 3:

Sample 3 Data Initial Conditions	
Height H_o (mm)	45.38
Volume V_o (mm³)	87506.78
Cross-sectional area (mm²)	1928.31
Weight of soil (g)	179.52
Specific Gravity G_s (g/cm3)	2.66
Natural density (g/cm³)	2.05
Dry density (g/cm³)	**1.77**
Moisture content w (%)	**15.84**
Volume of Solids Vs (mm³)	56981.36
Volume of Voids Vv (mm³)	30525.42
Void ratio	0.54
Vw (mm³)	24008.75
Degree of Saturation Sr (%)	78.65

Table 5.2.5: *Test 3: Initial conditions*

Test 3 has a moisture content below that of the calculated optimum, and therefore can be said to have been compacted on the 'dry' side. Its dry density as expected is similar to that of the optimum, but slightly lower, as can be seen from figure 5.1.1.

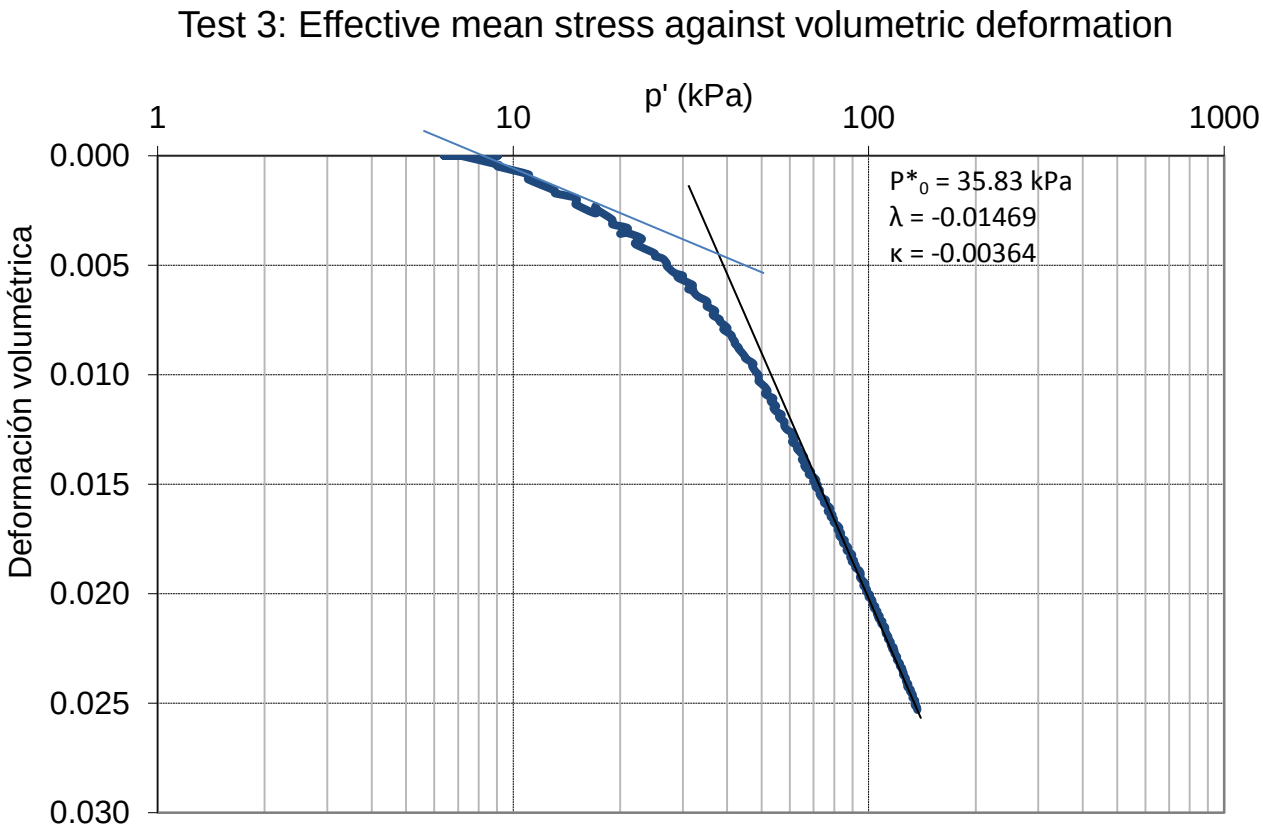

Figure 5.2.7: *Test 3: Effective mean stress against volumetric deformation*

Figure 5.2.7 shows the effective mean stress against volumetric deformation relationship for test 3. This test was not extended to stress levels as high as the two previous tests, causing a less extended curve, as discussed later.

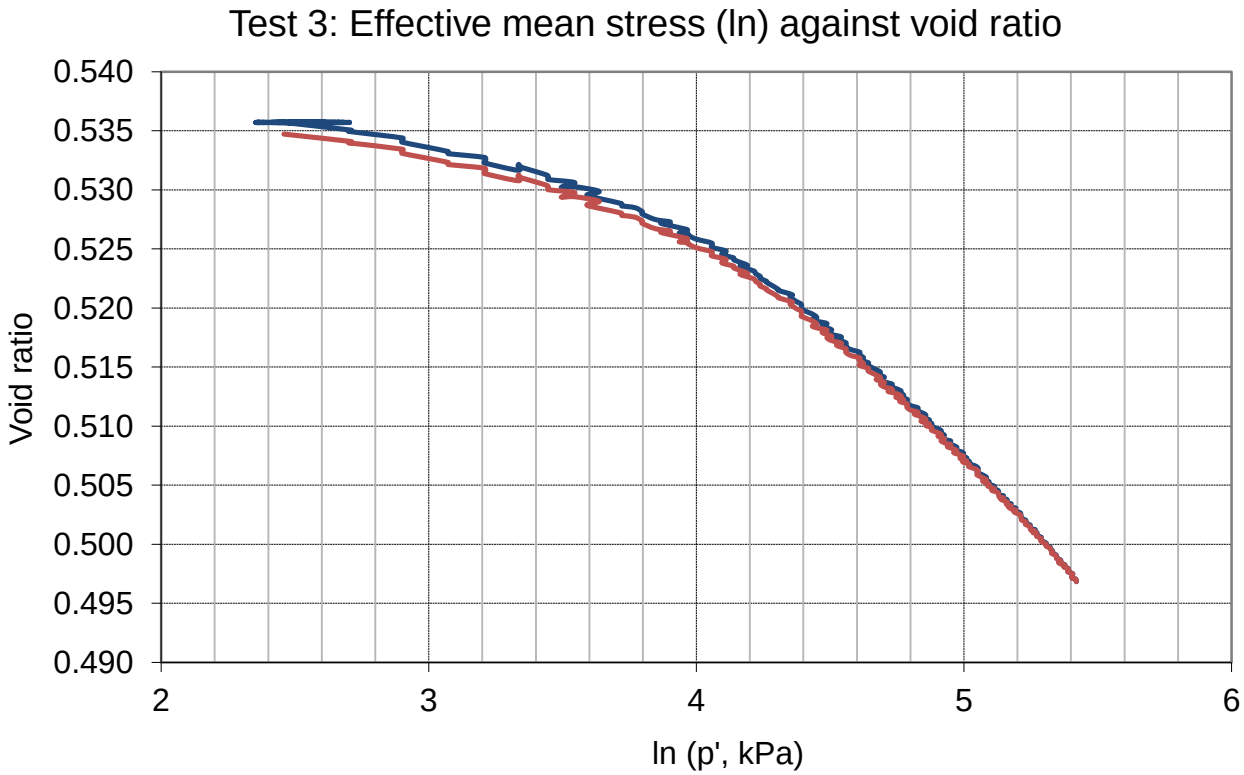

Figure 5.2.8: *Test 3: Effective mean stress (ln) against void ratio*

Figure 5.2.8 shows the measured change in void ratio for test 3 as 0.001. This value is insignificant in comparison to the overall void ratio of the sample, and can therefore be ignored.

Graphical parameters:

λ	κ	P_o^*
-0.01469	-0.00364	35.83 kPa

Table 5.2.6: *Test 3: Graphical parameters*

Both the slope of the recompression and virgin compression lines are lower than those of the previous two tests, giving a preconsolidation stress much lower than tests 1 and 2. This could indicate a significant reliance on the moisture content parameter, as the dry density parameter for test 1 and test 3 is very similar, or possibly an issue with the validity of the results due to the short period of testing time.

The compression phase of test 3 was continued to a radial pressure of around 180kPa, as shown by figure 5.2.9. The test was stopped due to issues with the machinery, but the results were considered as being suitable for use.

The pore pressure was measured as practically constant, making the effective and total radial stress paths equal in slope, and the test as a whole in fully drained condition

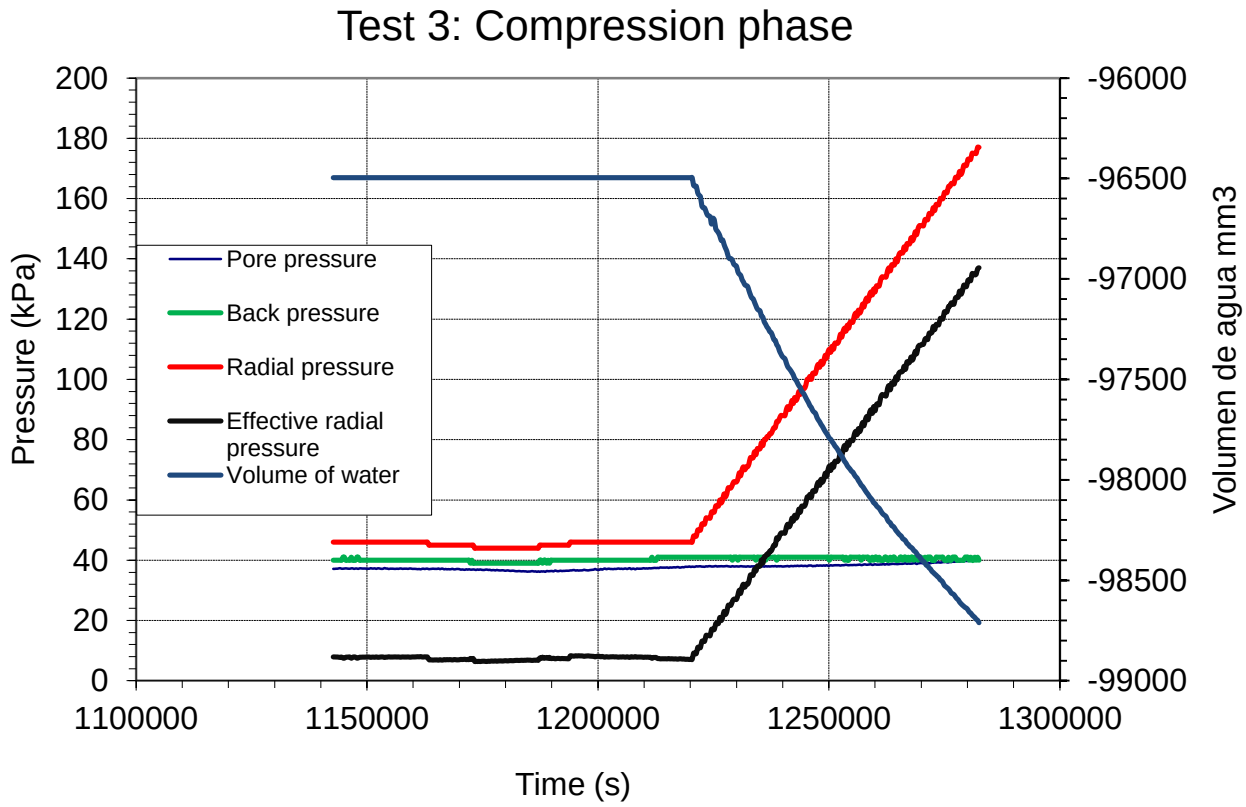

Figure 5.2.9: *Test 3: Compression phase process*

5.2.1.4 Test 4

Initial conditions of test 4:

Sample 4 Data Initial Conditions	
Height H_o (mm)	67.48
Volume V_o (mm³)	134411.49
Cross-sectional area (mm²)	1991.87
Weight of soil (g)	288.74
Specific Gravity G_s (g/cm3)	2.66
Natural density (g/cm³)	2.15
Dry density (g/cm³)	**1.74**
Moisture content w (%)	**17.07**
Volume of Solids Vs (mm³)	108548.87
Volume of Voids Vv (mm³)	25862.62
Void ratio	0.2383
Vw (mm³)	49287.92
Degree of Saturation Sr (%)	190.58

Table 5.2.7: *Test 4: Initial conditions*

Test 4 is of moisture content 17.07%, the highest of the standard Proctor tests and therefore also on the 'wet' side of the optimum. The dry density of this sample is 1.74g/cm³.

The results for effective mean stress against volumetric deformation for the triaxial testing process are shown in figure 5.2.10.

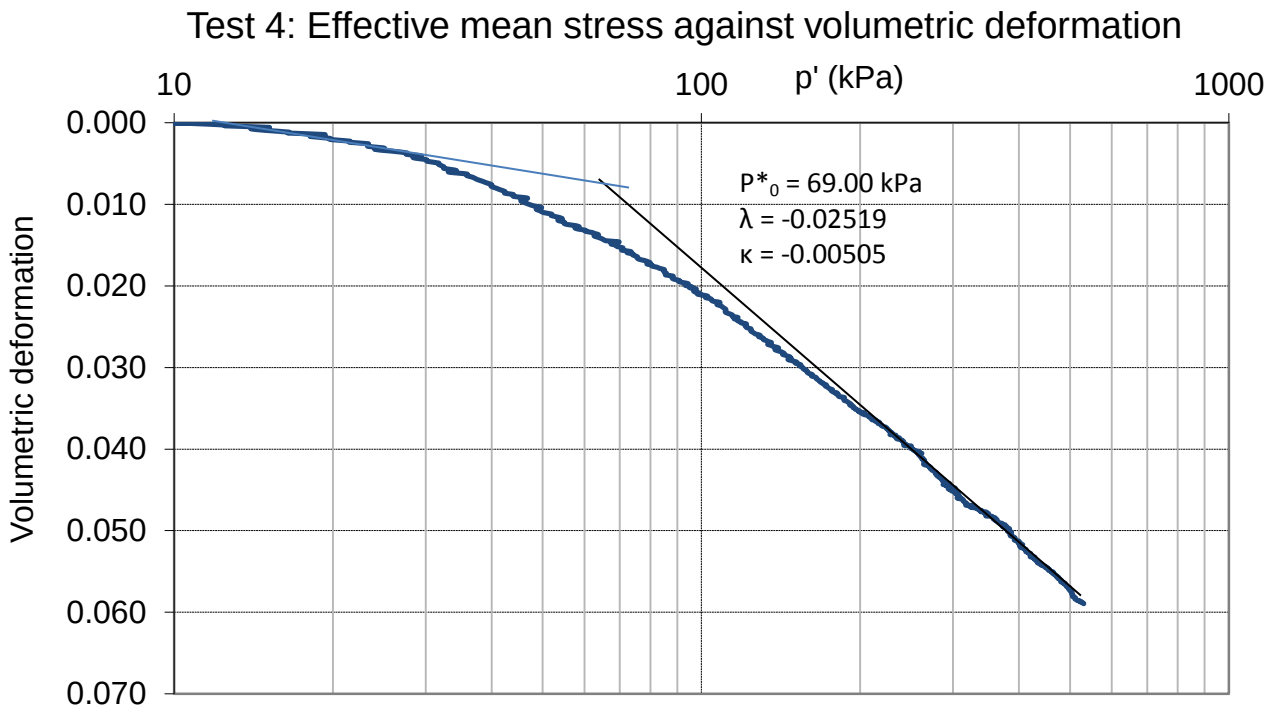

Figure 5.2.10: *Test 4: Effective mean stress against volumetric deformation*

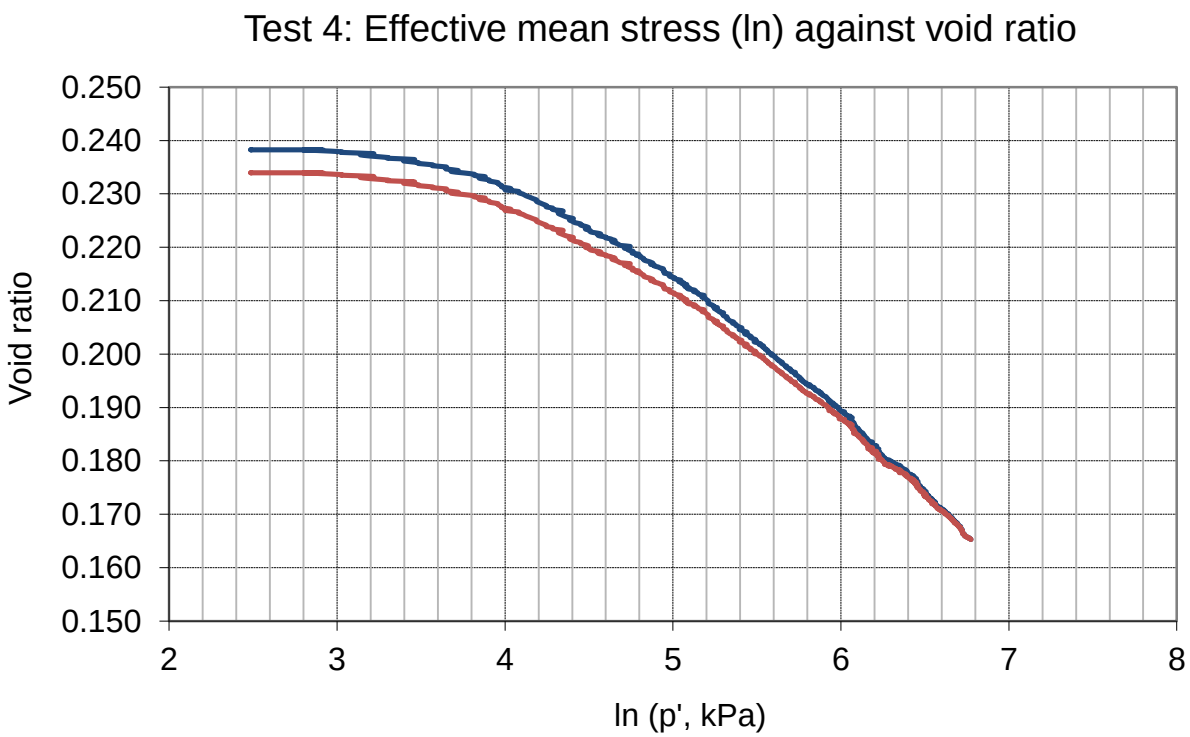

Figure 5.2.11: *Test 4: Effective mean stress (ln) against void ratio*

Figure 5.2.11 shows the change in void ratio associated with the trimming and saturation process as 0.0043. Again a small enough value to be ignored in terms of its affect on the preconsolidation stress

Graphical parameters for comparison:

λ	κ	P_o^*
-0.02519	-0.00505	69.00 kPa

Table 5.2.8: *Test 4: Graphical parameters*

Table 5.2.8 shows that the slope of the virgin compression and recompression lines is similar to those of tests 1 and 2, but the preconsolidation stress is significantly lower, suggesting the possible existence of a relationship due to the sample's increased moisture content.

The compression phase process is shown in figure 5.2.12. The radial pressure for test 4 was continued to around 600kPa, sufficient for both preconsolidation stress measurement and obtention of graphical parameters.

Some increase in pore pressure was experienced, but not significant enough to cause issues during testing or to alter significantly any results.

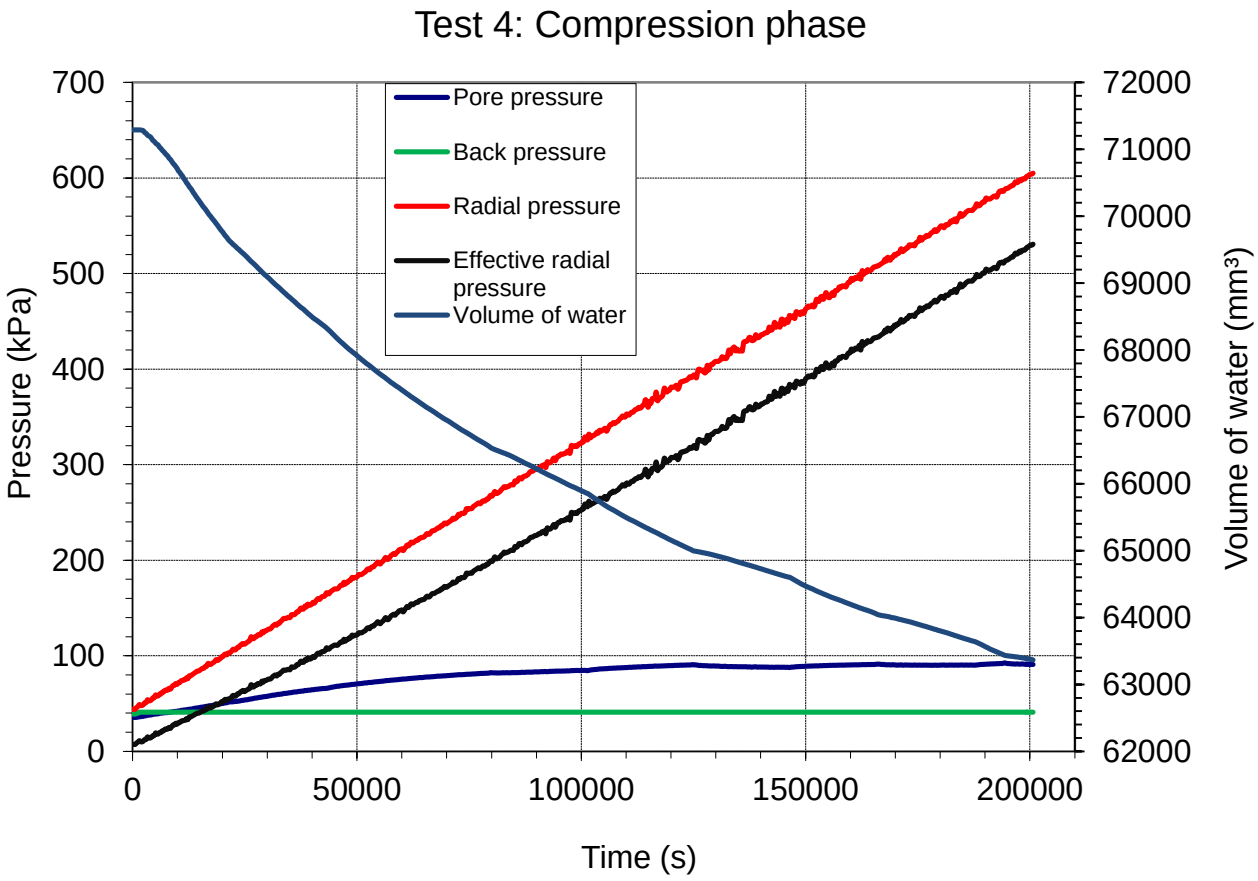

Figure 5.2.12: *Test 4: Compression phase process*

5.2.2 Half-force Proctor

Two tests were carried out using the half-force Proctor compaction method to then be used in triaxial compression testing. It may not be possible to determine a relationship from only 2 points, but some indication of the difference between the half-force Proctor results and the standard Proctor results, paired with the standard Proctor results themselves, may serve to come to some conclusion.

5.2.2.1 Test 5

Initial conditions of test 5:

Sample 5 Data Initial Conditions	
Height H_o (mm)	54.87
Volume V_o (mm^3)	109033.72
Cross-sectional area (mm^2)	1987.13
Weight of soil (g)	226.69
Specific Gravity G_s (g/cm3)	2.66
Natural density (g/cm^3)	2.08
Dry density (g/cm^3)	**1.71**
Moisture content w (%)	**16.77**
Volume of Solids Vs (mm^3)	72982.62
Volume of Voids Vv (mm^3)	36051.10
Void ratio	0.49
Vw (mm^3)	32556.23
Degree of Saturation Sr (%)	90.31

Table 5.2.9: *Test 5: Initial conditions*

The sample for test 5 has a moisture content of 16.77, above the optimum of 16.4 found for the half Proctor results, and can be described as being slightly on the 'wet' side. The corresponding dry density is 1.71.

The effective mean stress against volumetric deformation relationship is shown graphically in figure 5.2.13.

Figure 5.2.14 shows the change in void ratio associated with the trimming and saturation process as 0.0025, a value too small to have an impact on the preconsolidation stress parameter in the same way as the previous tests.

Graphical parameters:

λ	**κ**	**P_o^***
-0.0214	-0.00202	110.23 kPa

Table 5.2.10: *Test 5: Graphical parameters*

Table 5.2.10 shows the graphical parameters for test 5. The slope of the recompression line is found as relatively small, whereas the virgin compression line slope fairly similar to the standard proctor tests. The preconsolidation stress has been found as similar to but slightly lower than the value for test 2, of similar initial moisture content .

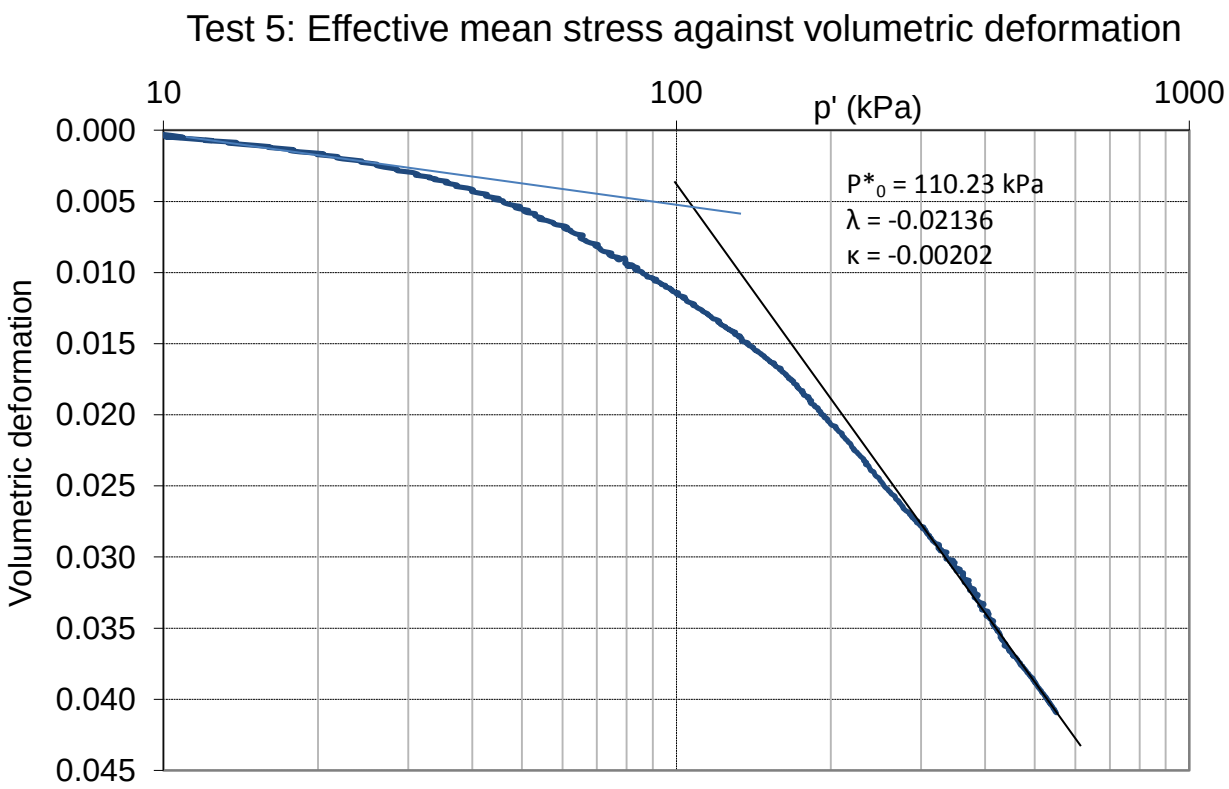

Figure 5.2.13: *Test 5: Effective mean stress against volumetric deformation*

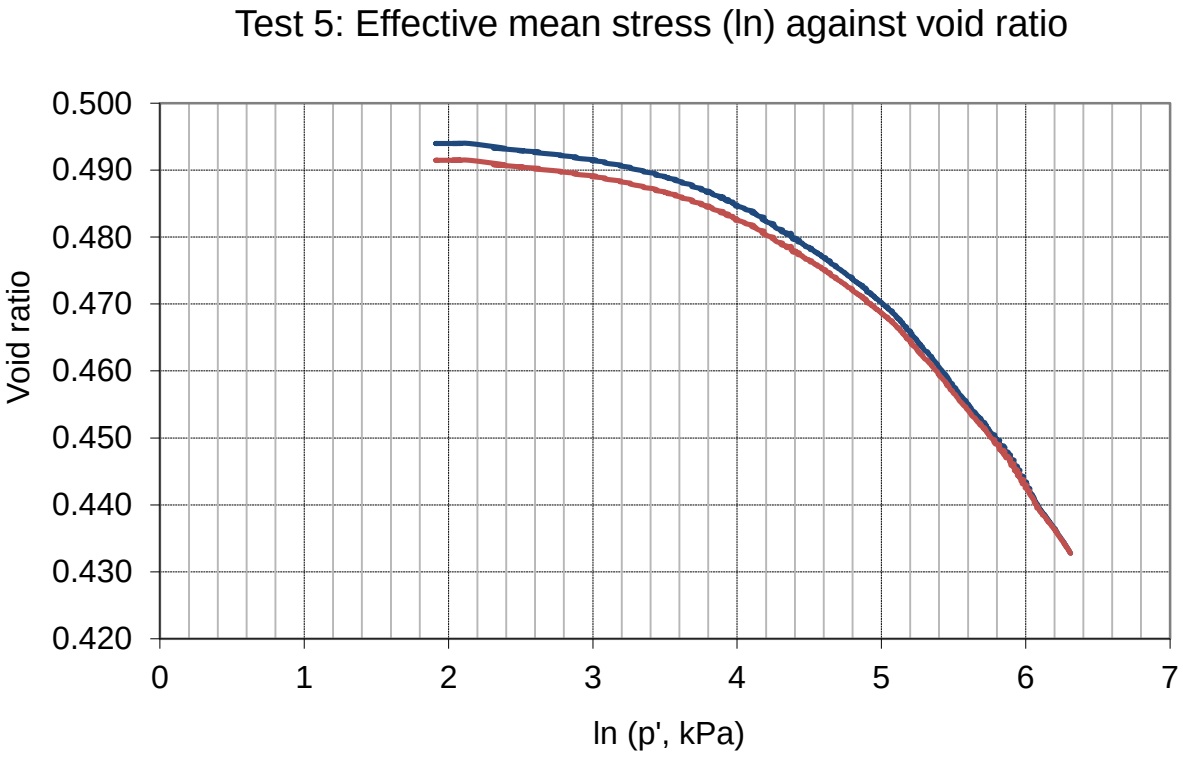

Figure 5.2.14: *Test 5: Effective mean stress (ln) against void ratio*

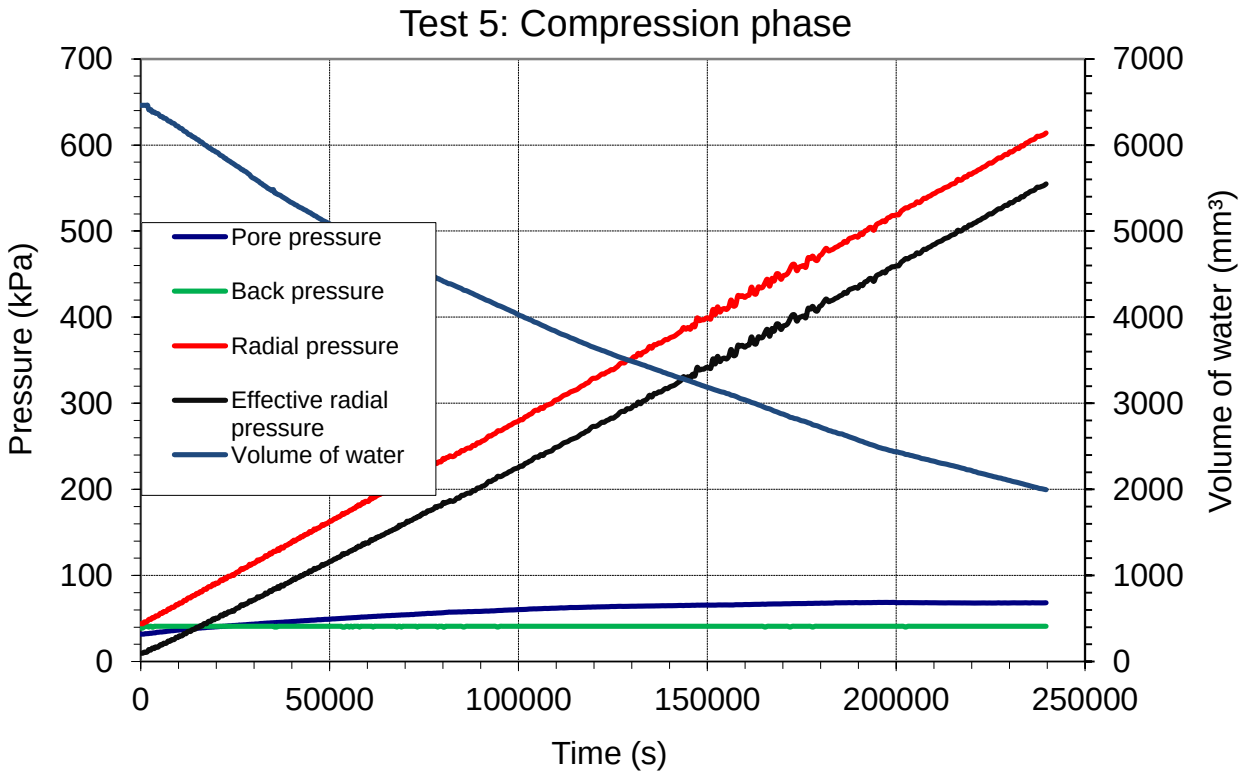

Figure 5.2.15: *Test 5: Compression phase process*

Figure 5.2.15 shows the compression phase process followed for test 5. Again the radial pressure was continued until around 600kPa to allow the collection of useful results.

The pressure ramp was applied slowly enough to produce only a small increase in pore pressure, making the use of the effective radial pressure results viable.

5.2.2.2 Test 6

Test 6 was carried out on a separate triaxial machine, capable of measuring the same parameters as that used for the other tests, but slightly less sophisticated. The results are still relevant, and all the necessary parameters can still be derived, but the appearance of the graphs is slightly different.

Initial conditions for test 6:

Sample 6 Data Initial Conditions	
Height H_o (mm)	53.26
Volume V_o (mm³)	59579.22
Cross-sectional area (mm²)	1118.65
Weight of soil (g)	114.77
Specific Gravity G_s (g/cm3)	2.66
Natural density (g/cm³)	1.93
Dry density (g/cm³)	**1.72**
Moisture content w (%)	**12.29**
Volume of Solids Vs (mm³)	43146.62
Volume of Voids Vv (mm³)	16432.61
Void ratio	0.3809
Vw (mm³)	14105.23
Degree of Saturation Sr (%)	85.84

Table 5.2.11: *Test 6: Initial conditions*

The sample for test 6 has a moisture content of 12.29%, clearly on the 'dry' side of the half-force proctor optimum. The corresponding dry density was measured as 1.72g/cm³

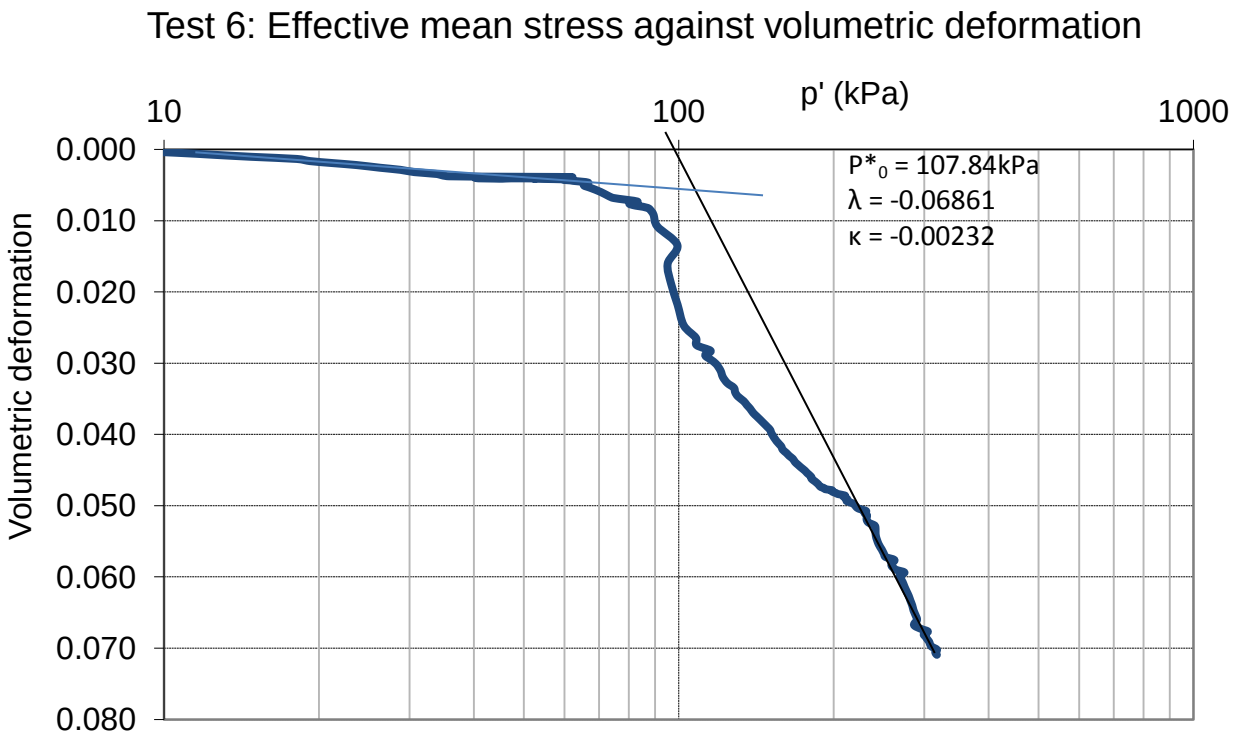

Figure 5.2.16: *Test 6: Effective mean stress against volumetric deformation*

Figure 5.2.16 shows the effective mean stress against volumetric deformation relationship for this test. The change in gradient between the recompression and virgin compression lines can be seen to be slightly more erratic than that of the previous tests, but levels out into a constant gradient, making the obtention of the preconsolidation stress parameter possible.

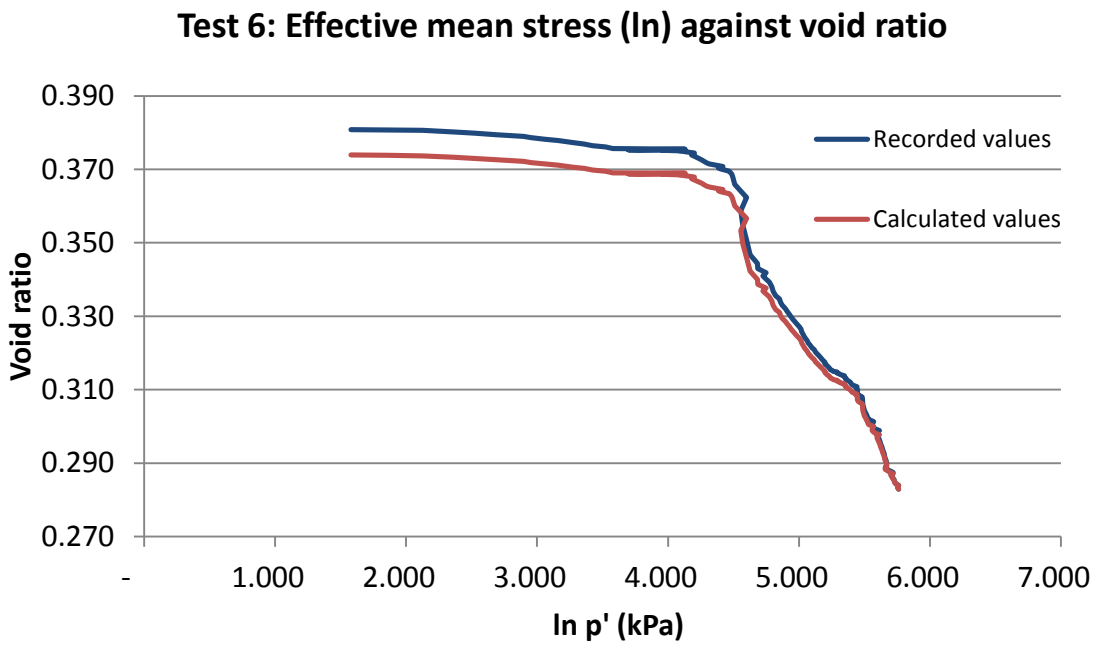

Figure 5.2.17: *Test 6: Effective mean stress (ln) against void ratio*

Figure 5.2.17 shows the change in void ratio associated with the trimming and saturation process as 0.0069, too small to cause any real change in the preconsolidation stress.

Graphical parameters:

λ	κ	P_o^*
-0.0686	-0.00232	107.84 kPa

Table 5.2.12: *Test 6: Graphical parameters*

Table 5.2.12 shows the graphical parameters for test 6. The recompression slope is similar to that of the other tests, but the virgin compression slope seems much steeper, indicating large deformations with small increases in effective mean stress. The preconsolidation parameter, however, is similar to that of test 5, the other half Proctor test.

Figure 5.2.18 shows the compression phase process for test 6. The data was recorded up to radial pressures of around 350kPa due to time restraints, but was sufficient for the derivation of useful parameters. As in test 3, the pressure ramp was applied slowly enough for fully drained conditions to ensue, and therefore the pore pressure within the sample to remain constant throughout the testing.

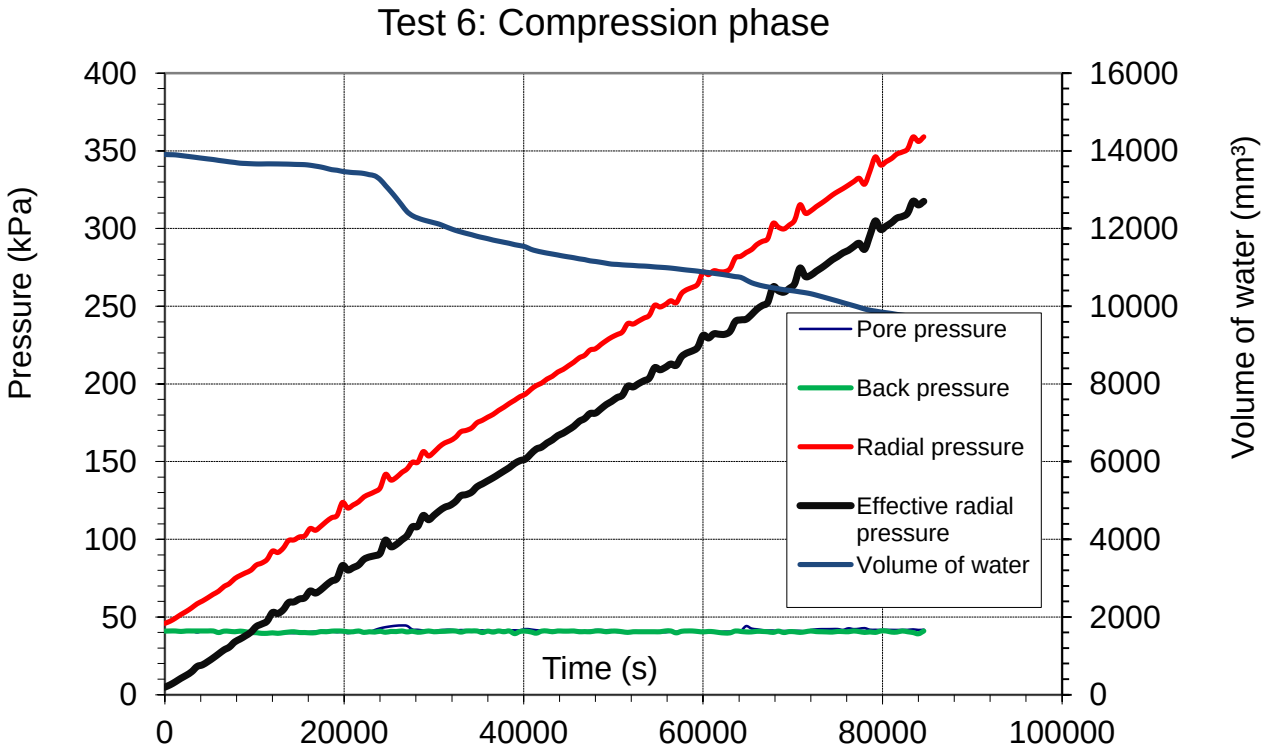

Figure 5.2.18: *Test 6: Compression phase process*

5.2.3 Permeability Calculations

For each of the triaxial tests, the permeability of the sample may be found using the recorded data to calculate the flow of water through the sample in constant conditions.

This is achieved by plotting the volume of water entering the sample against time during the initial saturation phase. Once this entry of water and therefore the gradient of this line becomes constant, the sample is fully saturated and its permeability can be calculated from the flow of water through the sample, taken as the amount of water entering the sample divided by the period of time taken to pass through. This flow value is multiplied by the grad h value, which itself calculated via the sample dimensions and input pressure value, in order to calculate the sample permeability.

For each of the graphs below, the red line indicates the constant flow of water used in the permeability calculations.

5.2.3.1 Test 1

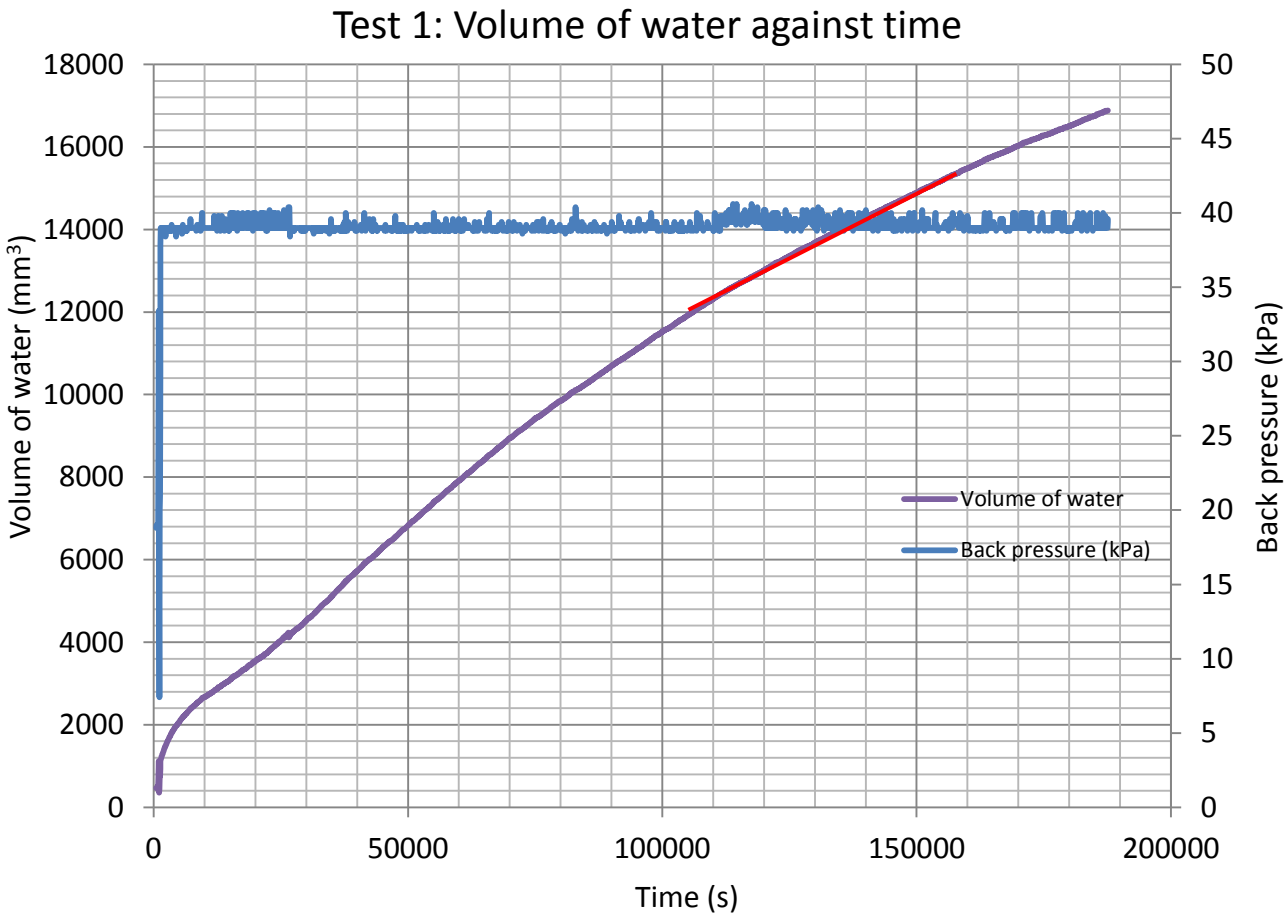

Figure 5.2.19: *Test 1: Volume of water against time*

Calculated permeability for test 1 = **9.68×10^{-10} ms^{-1}**

5.2.3.2 Test 2

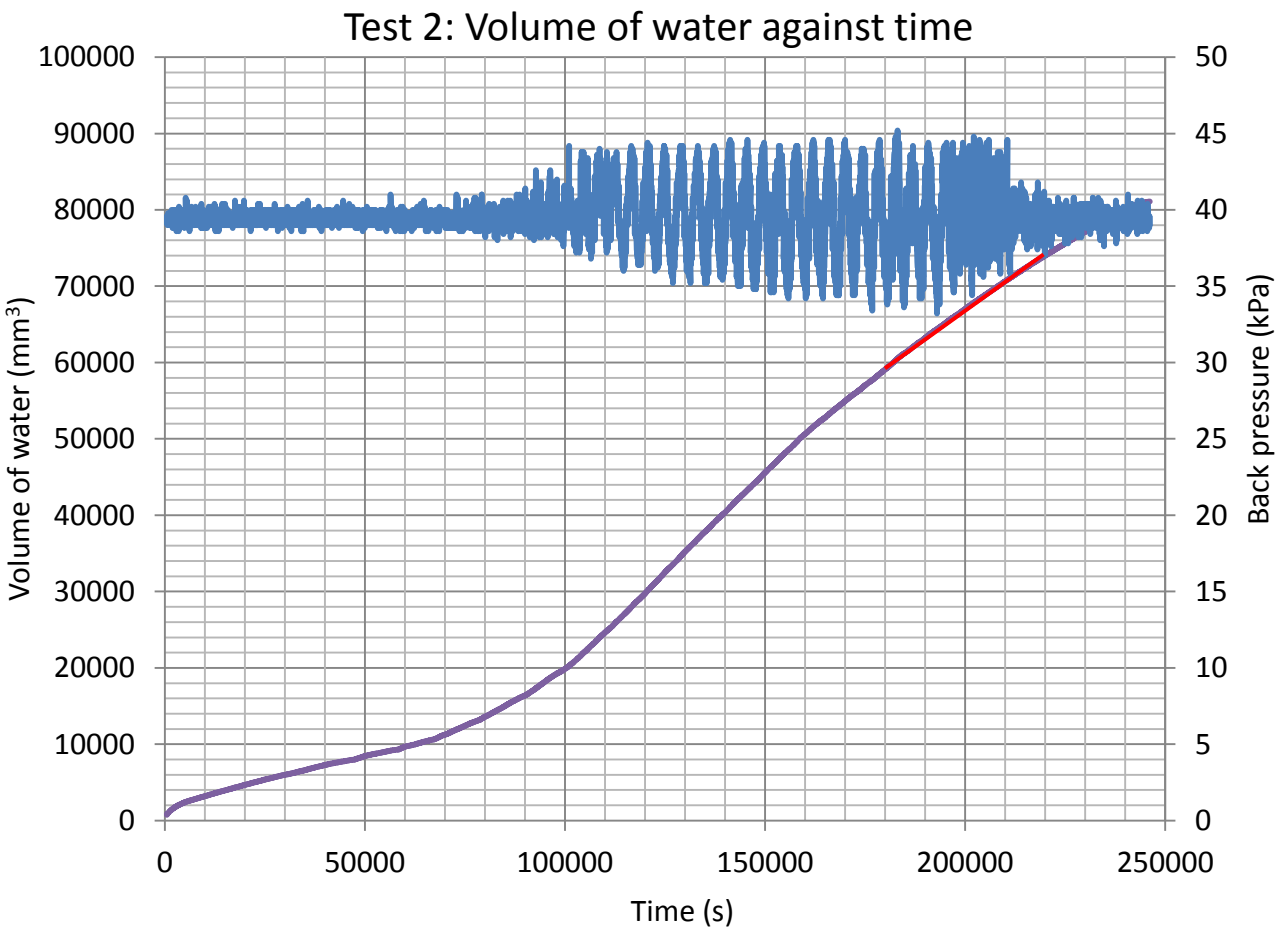

Figure 5.2.20: *Test 2: Volume of water against time*

Calculated permeability for test 2 = **3.49×10^{-9} ms^{-1}**

5.2.3.3 Test 3

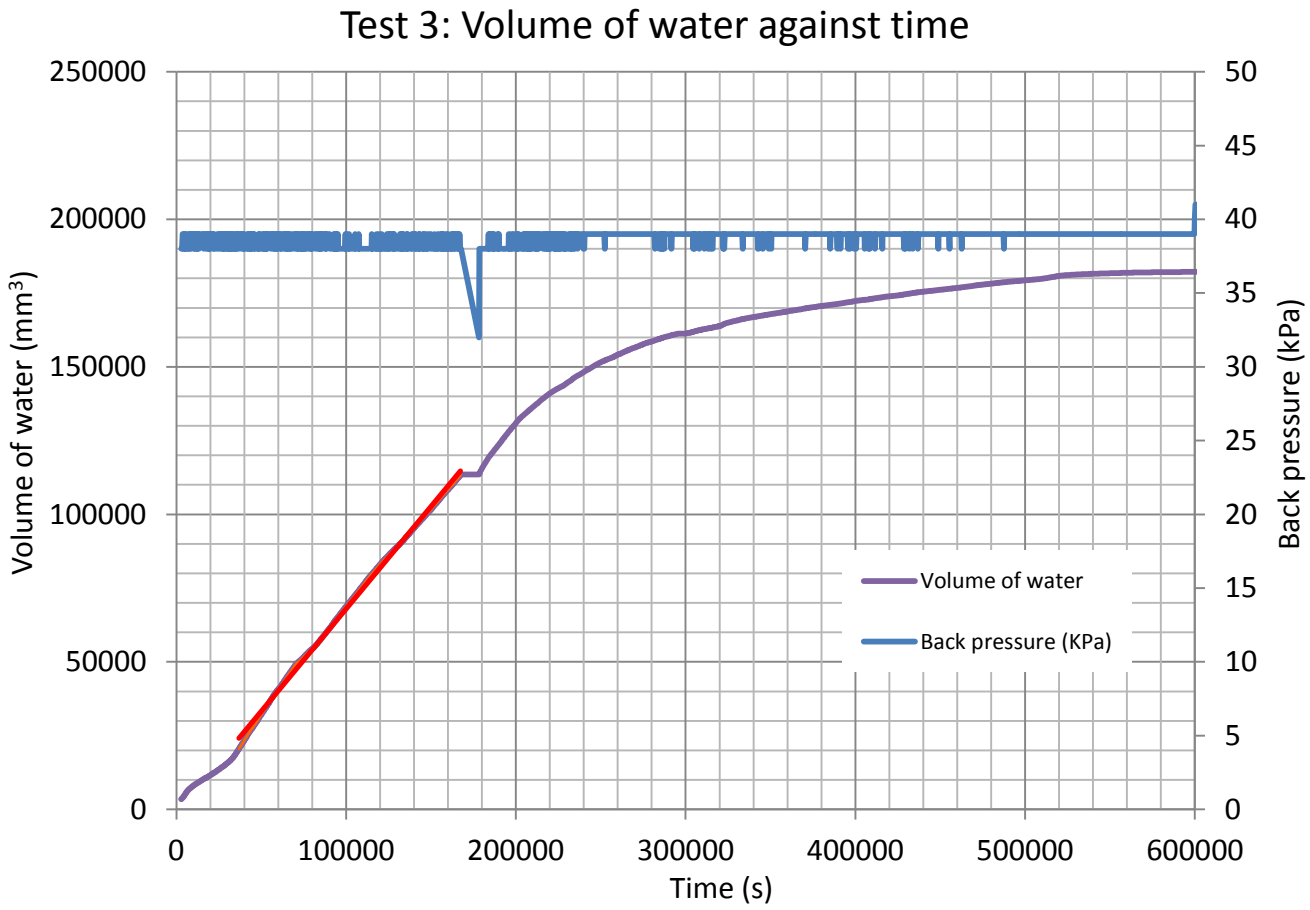

Figure 5.2.21: *Test 3: Volume of water against time*

Calculated permeability for test 3 = **4.35×10^{-9} ms^{-1}**

5.2.3.4 Test 4

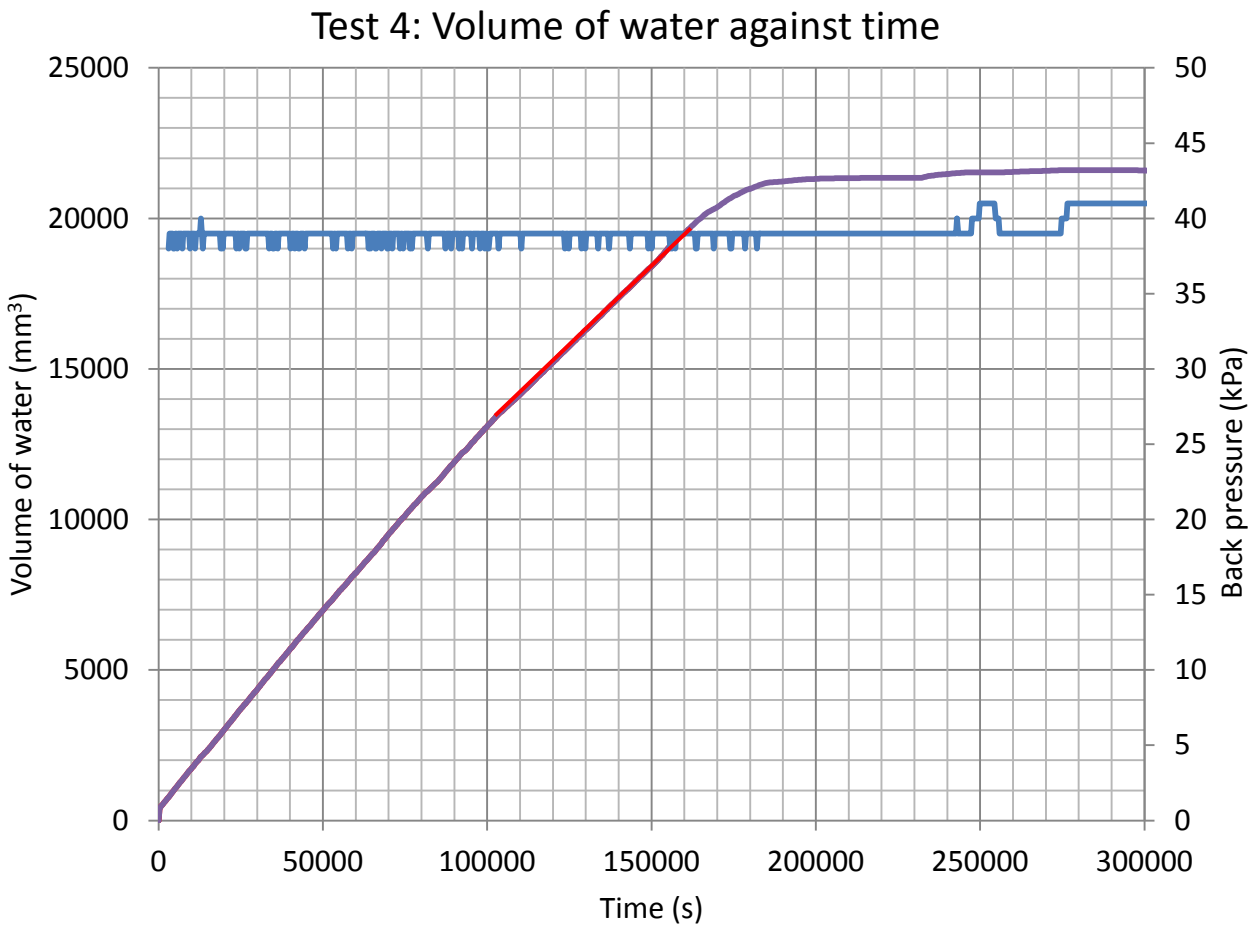

Figure 5.2.22: *Test 4: Volume of water against time*

Calculated permeability for test 4 = **7.32×10^{-10} ms^{-1}**

5.2.3.5 Test 5

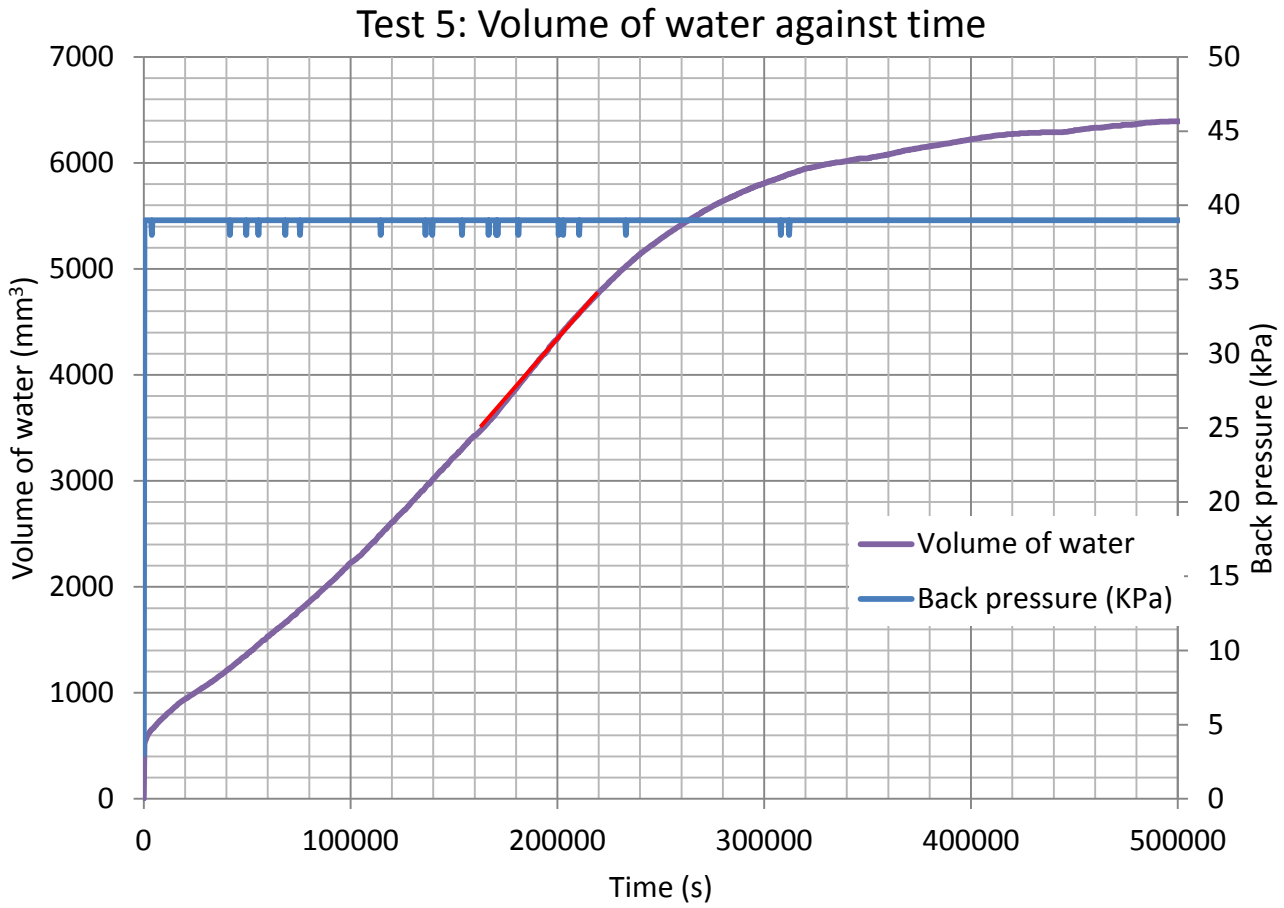

Figure 5.2.23: *Test 5: Volume of water against time*

Calculated permeability for test 5: **1.58×10^{-10} ms^{-1}**

5.2.3.6 Test 6

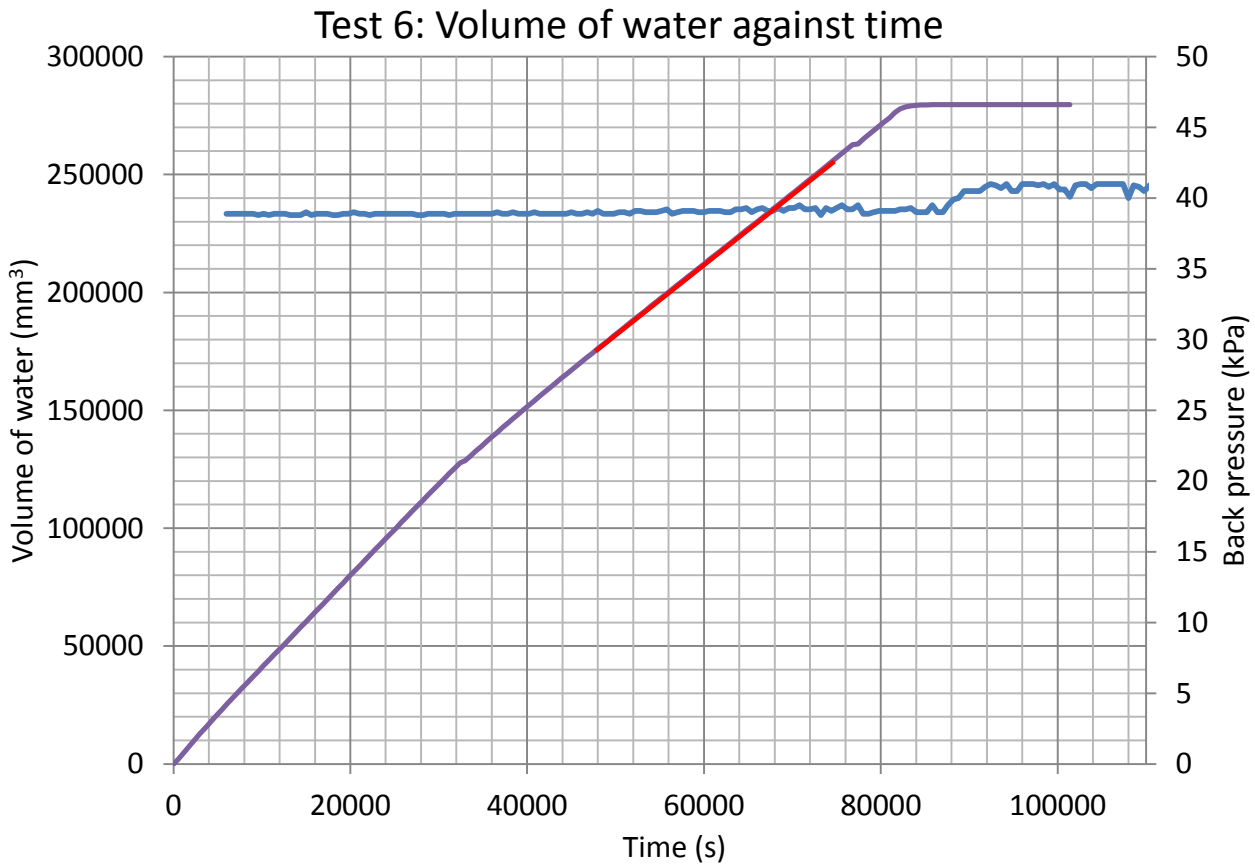

Figure 5.2.24: *Test 6: Volume of water against time*

Calculated permeability for test 6: **4.27×10^{-8} ms^{-1}**

5.2.3.7 Comparisons

Test no.	Compaction type	Permeability (ms^{-1})
1	Standard Proctor	9.68×10^{-10}
2	Standard Proctor	3.49×10^{-9}
3	Standard Proctor	4.35×10^{-9}
4	Standard Proctor	7.32×10^{-10}
5	Half Proctor	1.58×10^{-10}
6	Half Proctor	4.27×10^{-8}

Table 5.2.13: Comparisons of permeability of triaxial samples

The measured permeabilities for the samples vary between 9.68×10^{-10} to 4.27×10^{-8}

6 ANALYSIS

As the purpose of the paper is to attempt to determine a relationship for the saturated preconsolidation stress in terms of moisture content and dry density, this value is plotted against the two variables separately to analyse the results.

6.1 Preconsolidation stress against moisture content

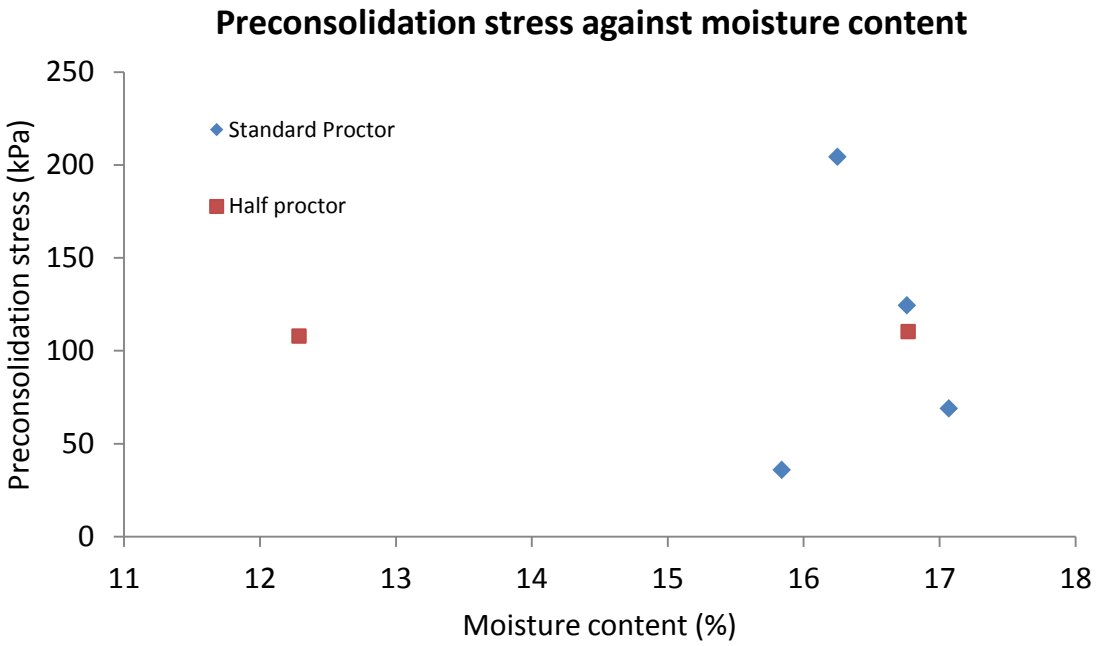

Figure 6.1.1: *Preconsolidation stress against moisture content*

Figure 6.1.1 shows the preconsolidation stress changes with changes in moisture content for the two types of compaction. From looking at the graph it can be seen that the value changes dramatically for varying values of moisture content, especially for the standard Proctor results.

As there are only two points for the half Proctor results, it would be more useful to separate the standard Proctor graph for further analysis.

Figure 6.1.2 shows the separated results for those samples compacted using the standard Proctor method.

From the results gathered, three alternatives for the analysis of these results can be seen to exist.

6.1.1 Alternative 1

From figure 6.1.2 it can be seen that there is an apparent direct relationship between the preconsolidation stress and the initial moisture content. The curve of the graph appears to follow a similar path to the Proctor compaction curve, in that an ‘optimum’ moisture content can be derived, along with a maximum preconsolidation stress associated with it.

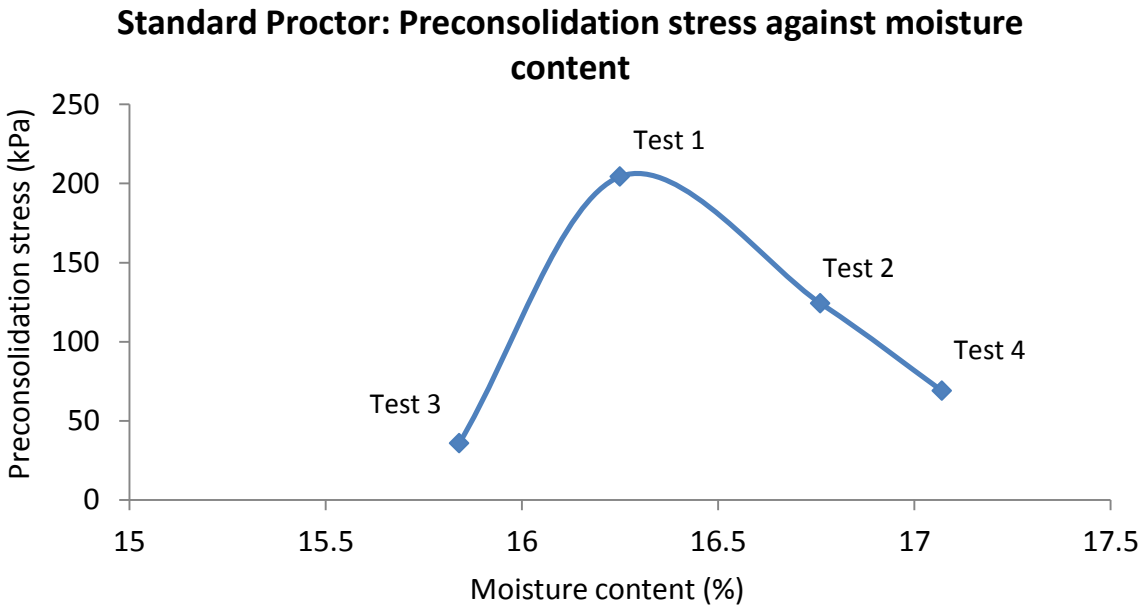

Figure 6.1.2: *Standard Proctor results: Preconsolidation stress against moisture content alternative 1*

Assuming that the apparent relationship shown by figure 6.1.2 exists and is true, the theoretical 'optimum' moisture content can be seen to be around 16.3%, which results in a maximum preconsolidation stress of around 208kPa.

However, The two half-force Proctor results, of very different moisture contents, give similar values for the preconsolidation stress, which implies that if an optimum style relationship does exist, the slope must be much smoother than that given in figure 6.1.2.

From figure 6.1.2 alone it can be said that whatever relationship may exist seems to respect the existence of an optimum moisture content, for which the preconsolidation stress is at a maximum.

6.1.2 Alternative 2

Due to the comparatively low pressure ramp that was applied during test 3, it is possible that the preconsolidation pressure was miscalculated, and that this result is therefore erroneous. If this is the case, a linear style relationship can be derived from the standard Proctor results, as shown by figure 6.1.3.

There is a possibility of this being the case, as the gradient of the graph comparing effective mean stress against volumetric deformation (displayed in figure 5.2.7) may not have become constant at the section from which the λ value was taken. i.e. the preconsolidation stress may not have been passed during testing, or if so only just, making the process to graphically derive its value incorrect.

This relationship would match with the expected results from earlier. However, the slope of the line describing this relationship is very steep, which would suggest very large apparent preconsolidation pressures for low values in moisture content.

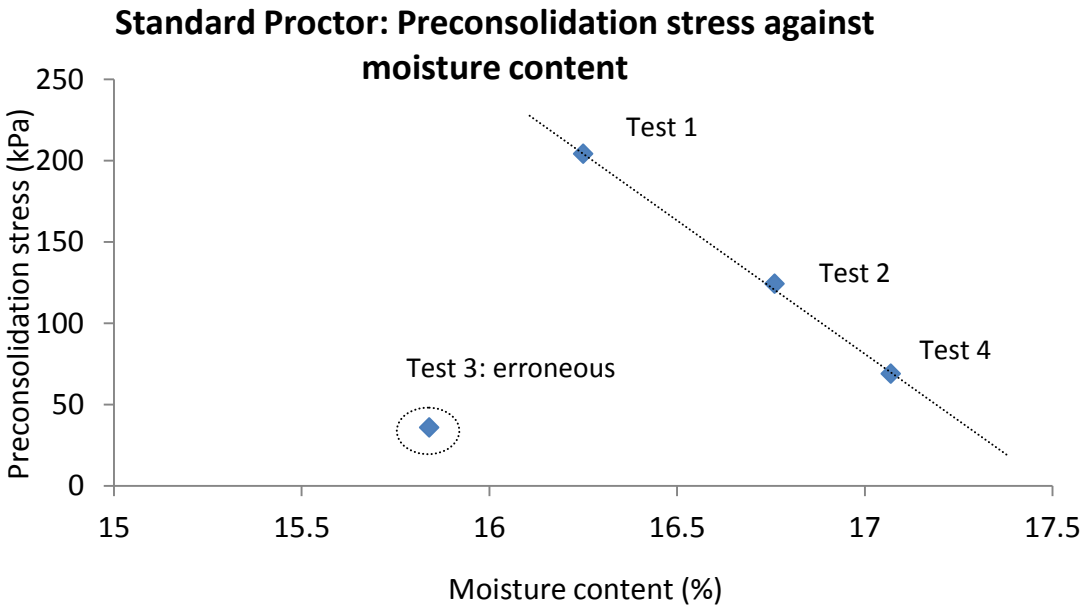

Figure 6.1.3: *Standard Proctor: Preconsolidation stress against moisture content alternative 2*

6.1.3 Alternative 3

The moisture contents only vary over a small range, but seem to induce very large changes in the preconsolidation stress. It is possible that the results do not follow an 'optimum style' pattern or a linear pattern at all, but are in fact randomly distributed throughout the graph. The only way to test this theory would be to carry out more experiments, following the same procedure but using a wider range of moisture contents.

6.2 Preconsolidation stress against dry density

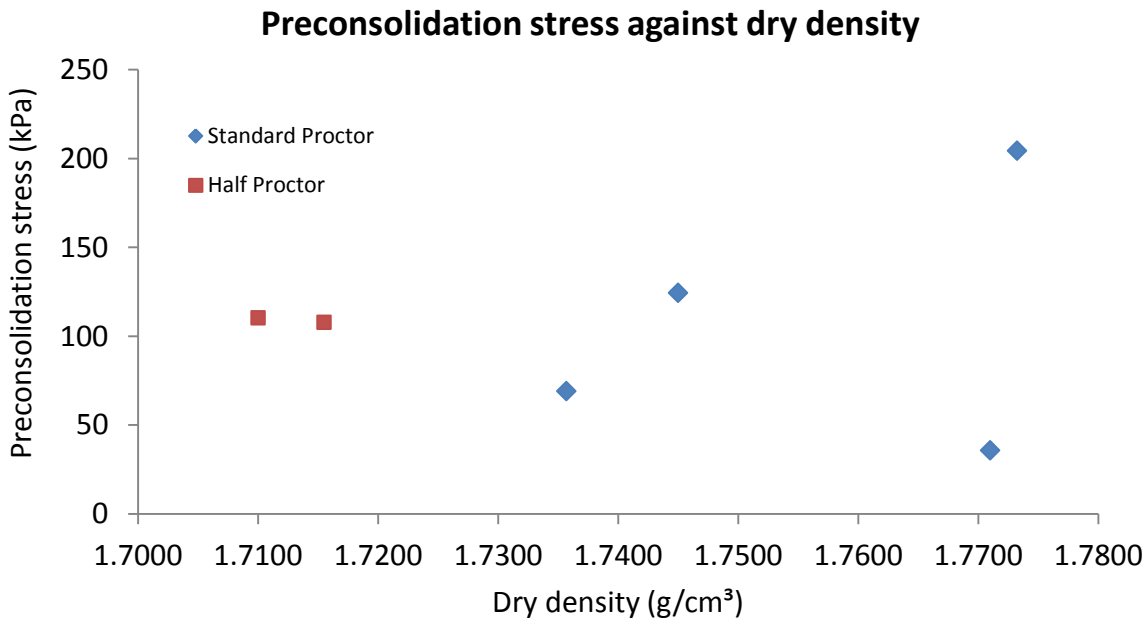

Figure 6.2.1: *Preconsolidation stress against dry density*

Figure 6.2.1 shows the values for preconsolidation stress plotted against dry density for all 6 tests. From initial viewing of the graph, there does not seem to be any decipherable relationship. Like with the comparison against moisture content, the standard Proctor compacted results alone could be more useful.

Figure 6.2.2 shows the standard Proctor compacted results for preconsolidation stress plotted against dry density. Using all the data points, no direct or useful relationship seems to exist, however, two alternatives can be considered:

6.2.1 Alternative 1

By following the same method as for alternative 2 comparing preconsolidation stress and moisture content and taking test 3 as being erroneous, it is possible to come up with a linear-style relationship between the results, as shown by figure 6.2.2.

However, this relationship is brought into question by two data points of the half-proctor results, which seem to yield no apparent direct relationship. If a linear relationship did exist, it is likely that it would also be shown by the two half-force Proctor results as well.

6.2.2 Alternative 2

A second alternative is that there is in fact no direct relationship between the preconsolidation pressure and the dry density, and that the changes can only be mapped indirectly with respect to the parameter's dependency on the moisture content and by the moisture content's relationship with the dry density, should that relationship itself exist.

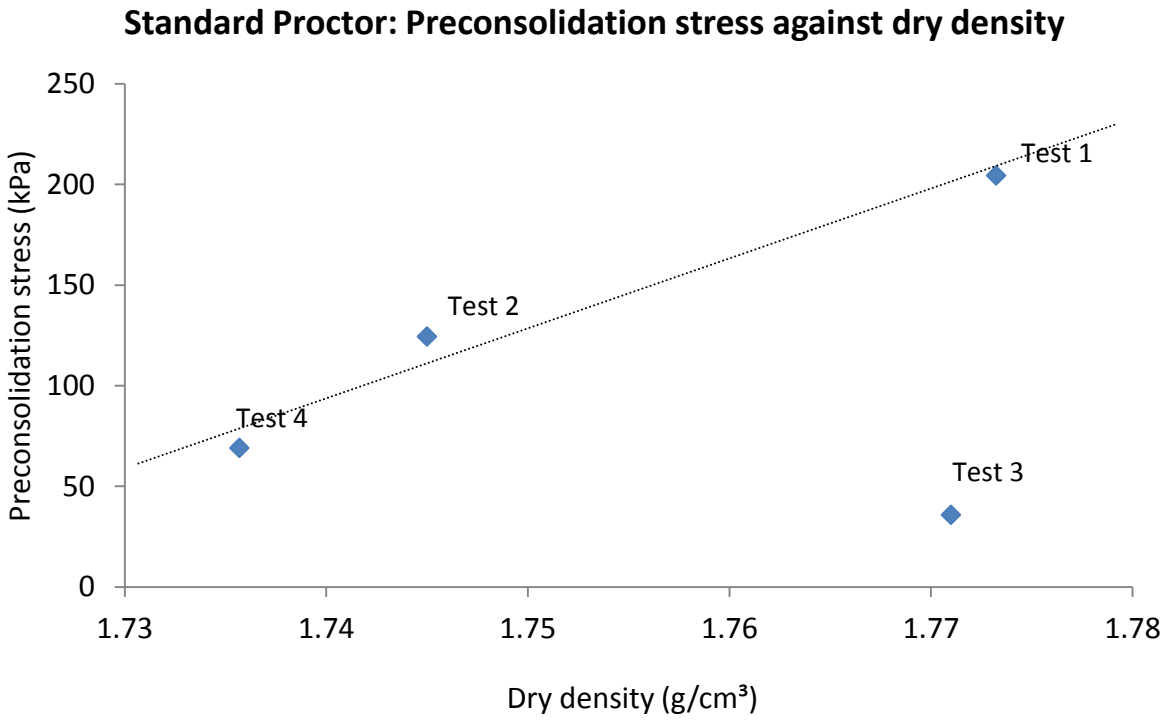

Figure 6.2.2: *Standard Proctor: Preconsolidation stress against dry density alternative 1*

6.3 Comparative parameters

Test no.	Compaction type	w (%)	ρ (g/cm³)	λ	κ	p_0^* (kPa)
1	Standard Proctor	16.25	1.77	-0.0322	-0.00460	204.38
2	Standard Proctor	16.76	1.75	-0.0181	-0.00723	124.39
3	Standard Proctor	15.84	1.77	-0.0147	-0.00364	35.83
4	Standard Proctor	17.07	1.74	-0.0252	-0.00505	69.00
5	Half Proctor	16.77	1.71	-0.0214	-0.00202	110.23
6	Half Proctor	12.29	1.72	-0.0686	-0.00232	107.84

Table 6.3.1: *Table of comparative parameters*

Table 6.3.1 shows a summary of the main variables used in this thesis. The initial moisture contents and dry densities of each of the tests, along with the resulting values for preconsolidation stress are shown. Also displayed are the values for the gradient of the two lines of the effective mean stress against volumetric deformation, the virgin compression and recompression lines.

This table is to be used for easy reference purposes and for use as a quick comparison between the tests and their results.

7 CONCLUSIONS

From the tests undertaken and the subsequent results recorded, several conclusions can be made concerning the obtention of the saturated preconsolidation stress of the A-28 clayey silt.

7.1 Preconsolidation stress relationships

The objective of the paper was to investigate the possibility of the existence of a direct relationship between the value for the saturated preconsolidation stress p^*_0 and both the moisture content w and the dry density ρ_d.

To attempt to achieve this aim, at least 8 experiments were planned to map the changes in this value for two types of compaction: Standard Proctor and half-force Proctor. Due to issues in testing, only 6 tests were achieved, 4 for Standard Proctor and 2 for half-force Proctor, making definitive conclusions difficult to achieve. However, from the Standard Proctor test results at least, some speculative conclusions may be drawn as to the nature of a possible preconsolidation stress relationship.

Two alternatives for an existing relationship between the preconsolidation stress and the moisture content have been found.

1. As shown by figure 6.1.2, in which the relationship is seen to follow a curve with an optimum point (with a corresponding maximum preconsolidation stress)

2. As demonstrated in 6.1.3, by discounting the result of test 3 (with reasoning) a linear relationship between the two can be shown, in which the preconsolidation stress can be seen to decrease with increases in moisture content.

Only one possible existing relationship has been found from the collected data between the preconsolidation stress and the dry density parameter:

1. As shown in figure 6.2.2, also by discounting the test 3 result, a linear relationship can be seen in which the preconsolidation stress increases with increasing dry density

However, for both of these relationships, there remains the possibility of no real correlation existing, and further testing is recommended before any concrete conclusion is founded.

7.2 Additional testing

It is clear that for any definitive trend to be derived, or for a complete conclusion regarding the existence of a relationship involving these parameters, extended testing involving samples of differing initial conditions is needed. The experiments and results given in this paper may be extended upon to achieve a more complete investigation.

The recommended extended testing that would result in a more complete conclusion is to repeat the Proctor compaction and triaxial compression testing to obtain at least 2 more preconsolidation stress data points for the standard Proctor test results, using moisture contents lower than 15.84% (of test 3). For the half-force Proctor, at least one intermediate data point between the existing two moisture content results, and a further 2 points at moisture contents higher than 16.77% (of test 5) would be sufficient to test the existence of any relationship

It would also be beneficial to plot the resulting dry densities of these additional tests on the existing graph of preconsolidation stress against dry density, to enable a final conclusion on the existence of a relationship to be made.

7.3 Change in void ratio due to trimming and saturation process

From the graphs comparing the changes in void ratio recorded by the GDSLAB monitoring equipment and those back-calculated using the final values and common soil mechanics formulae, the following can be concluded:

Although the soil trimming process and saturation process under constant cell pressure do cause a slight decrease in void ratio, this change is insignificant in its effect on the preconsolidation stress value for the sample being tested. In some experimentation in which the value for void ratio is deemed paramount, and in which accuracy is vital, this small change is almost certainly of importance. However, for the purposes of this paper, its effects are negligible.

8 Bibliography

E.E ALONSO, A. GENS, A. JOSA. (1990). A constitutive model for partially saturated soils. *Geotecnique* , 405-430.

R, GOMEZ. (2009). *CARACTERIZACIÓN HIDRO-MECÁNICA DEL SUELO DELTERRAPLÉN EXPERIMENTAL DE ROUEN.* Barcelona.

Allco. (2006-2010). *The importance of backfill confinement.* Retrieved June 17, 2011, from allco.co.nz: http://www.allco.co.nz/Our+Most+Requested+Drawings/Technical+Reference+205.html

Civil craft structures. (2010, March 15). *Phase relationships of Soil.* Retrieved June 19, 2011, from civilcraftstructures.com: http://www.civilcraftstructures.com/civil-subjects/phase-relationships-of-soil/

Industrial and Scientific Spares. (2010). *Proctor Compaction Apparatus.* Retrieved June 17, 2011, from Industrialscientific.in: http://www.industrialscientific.in/proctor-compaction-apparatus.htm

IOWA Department of Transportation. (1999, October 26). *METHOD OF TEST STANDARD PROCTOR MOISTURE DENSITY RELATIONSHIP OF SOILS FIELD PROCEDURE FOR LABORATORY TEST METHOD 103.* Retrieved June 16, 2011, from www.iowadot.gov: http://www.iowadot.gov/erl/archives/Apr_2004/IM/content/309.pdf

Zeal International. (2009). *Zeal International.* Retrieved June 15, 2011, from zealinternational.com: http://www.zealinternational.com/soil/zi3041.asp